Master's thesis

NTNU
Norwegian University of Science and Technology
Faculty of Medicine and Health Sciences
Kavli Institute for Systems Neuroscience

Ingemars Sokolovskis

TAU-COUPLING BETWEEN BRAIN ACTIVITY PATTERNS AND FINGER MOVEMENTS IN ADULTS DURING AN INTERCEPTION TASK

Master's thesis in Neuroscience
Supervisor: Professor Audrey van der Meer
November 2021

NTNU
Norwegian University of
Science and Technology

Ingemars Sokolovskis

TAU-COUPLING BETWEEN BRAIN ACTIVITY PATTERNS AND FINGER MOVEMENTS IN ADULTS DURING AN INTERCEPTION TASK

Master's thesis in Neuroscience
Supervisor: Professor Audrey van der Meer
November 2021

Norwegian University of Science and Technology
Faculty of Medicine and Health Sciences
Kavli Institute for Systems Neuroscience

NTNU
Norwegian University of
Science and Technology

Abstract

High-density electroencephalography (EEG) was used to investigate Tau coupling between brain activity patterns and finger movements while adults were intercepting a moving target. EEG data for 12 participants were recorded with an array of 256-channel sensors. Adults were presented with an interception task, which consisted of a target car, moving towards a catching area at three different speeds and an effector dot to catch the car in the designated area with the motor movement of the finger. Tau-coupling, a part of general τ (tau) theory, helps to understand guiding movement by controlling the closure of gaps between effectors and their goals, was used in this study. By exploring the concept of resonance, on the foundation of radical embodiment, we took a closer look of dynamics of both neural and environment scale in relation to tau-coupling. Movement related potentials (MRPs) and visual evoked potentials (VEPs), and intrinsic tau-coupling were analysed. MRP and VEP analyses showed a main effect of target speed, indicating that N200 and P300 latencies for motion increased significantly with the speed of the moving object, as well as an observation of peak latencies always being longer in MRPs than VEPs. Tau-coupling analyses showed statistically significant results in slow, medium and fast speed conditions between car motion and finger movement coordinates, brain activity and car movement coordinates, brain activity and finger movement coordinates, and MRP & VEP average latency peaks. Tau-coupling analyses showed a main effect of speed, indicating that K-values of the slope increased with the speed of the moving object. It was concluded that Tau-coupling exists between visual perception, motor evoked potentials, finger movements and car movements in an interceptive timing task.

Keywords: Tau-coupling, EEG, visual evoked potentials, movement related potentials

Acknowledgements

The experimental work and writing was done at the Developmental Neuroscience Laboratory (Nu-lab), at the Norwegian University of Science and Technology (NTNU). Most of the planning and the beginning of the thesis was carried out at the Kavli Institute for Systems Neuroscience, at the Norwegian University of Science and Technology (NTNU).

Firstly, I am eternally grateful to my supervisor, Professor Audrey van der Meer and Professor Ruud van der Weel for their support, guidance and passion for the project. I will never forget their encouragement and help in times when I caught myself discarding dozens of hours of work because something needed to be re-done. I will always remember the smiles on our faces, when I handed in the final results and said, *"It's looking really good now, I think we did it!"*

Secondly, I would like to thank all of the current and previous members of Nu-lab for constantly helping with technical and theoretical questions, and motivating one another when times seemed rough. The laughs, the friendships, the coffee breaks and silly conversations truly helped.

Lastly, a deep sense of gratitude goes to my family and closest friends who believed in me when I said I was going to Norway to study Neuroscience. It turned out to be one of the toughest psychological challenges I had ever faced in my lifetime, and your light guided me through it.

This thesis represents a major milestone in my life; an opportunity that I had been dreaming about for many years. An opportunity that I will never forget and always be thankful for.

Riga, November 2021

Ingemars Sokolovskis

Table of contents

Introduction

Humans possess a remarkable ability of performing different motor actions, starting from simple ones like moving whole extremities to more difficult ones like simultaneously doing different small motor tasks with each hand. In order to do these tasks efficiently, a person must undergo different stages of learning, for example, gathering sensory information, previous experience, using decision making strategies and using neural representations of motor memory. Once all the components fall together and someone is ready to do a task, three classes of control are used to optimize motor performance and to perfect the task. Predictive control helps the feedback delays in the sensorimotor system and organizes previously learned information about the object or task; reactive control uses sensory inputs to update motor commands, while biomechanical control helps to control the necessary muscles (Wolpert, 2011).

Imagine a situation where you are standing in the middle of the basketball court, it is the last seconds of the game and the opponent has the ball. In order to win the game, they need to score three points by throwing a long pass over the whole court and making a shot as soon as possible. In your mind, you realize that the ball will fly over everyone's heads and land in someone's hands, but you have the task to intercept it. The referee blows the whistle and starts counting down the seconds to inbound, you see the opponent draw his hand back and throw the ball. At this moment as you see the ball fly all the way up in the air and get closer to your position, your brain starts calculating the potential trajectory, speed, and location where the ball will end up, as well as the motor response necessary to intercept its trajectory. At the same time, you start moving your extremities to run towards the potential position, and if your calculations were correct and if your athletic abilities allow you to surpass everyone else, you will succeed in intercepting the ball and winning the game. The perceptual prediction is an important aspect to understand the prospective guidance of movement. In different systematical environments, it is necessary to be able to predict the outcomes of action, which can be defined as affordances (van Andel et al., 2019). Affordances are relative and tied to individual persons or animals, based on their previous experiences, and in complex behavioral situations, they allow us to respond to the surrounding environment without constantly thinking of the outcome. Our neural system helps us to automatically break down the variables and efficiently understand which potential future actions may arise, resulting in a continuous perceptual exploration. Visual perceptual exploration is an important biological process that can be paralleled to animal (Gibson, 1958) and human

(Rushton et al., 1998) locomotion, where the visual system and motor movements join in a synergy. Our neural system organizes an efficient way to control exploratory movements and minimizes the metabolic cost of unnecessary movements, which helps us to carry out tasks more efficiently the more we practice them or if we have done something similar in our past. Previous research done by David Lee shows that this efficient way can be achieved by the neural system's reliance, as well as the direct guidance of movement through the perception of specifying optical variables (Lee, 1998).

In case of an interception task with a moving target, there is a need for prospective guiding of actions and perception. Interception tasks are cognitively demanding and require high spatial and temporal precision. Even though much is known about perception and motor skills, not a lot is known about neuronal mechanisms of interceptive actions, but researchers conclude that interception is regulated by repeatedly updated prediction of targets position and velocity in the specific setting (Brenner, 2018). The guiding of actions means that there is a need for a precise and calculated contact with the effector, which is the controlled object that collides with the moving object, i.e. hands when catching the basketball. Not only the controlled contact is important, but also how the force is applied and controlled from the effector to the object (Lee, 2001a). The prospective guiding of effector towards the object with the right settings – speed, velocity, time and place, require a coinciding regulation of rates of closure until they decrease to zero, such as the spatial gap among the effector and incoming object, between the effector and the location of the interception destination, as well as the gap between starting and end body postures that are required to intercept the object until contact is made (Lee, 2001a). In his earlier research, Lee explains an example of how a person who is driving a car and then braking, is regulating the braking in their brain with a single optical variable "Tau" (Lee, 1976), which can be taken as a starting point that sets the base tone for this paper. The discovery of tau helped to better understand the regulation of movement in various situations and animal species. Lee with his colleagues found that the tau variable was used in the landing behaviour of pigeons (Lee, 1993), the closing of the wings of plummeting gannets to control their movement (Lee, Reddish, 1981), and as a strategy for human long-jumpers to regulate their running approach on the track (Lee et al., 1982). Lee's research on tau led him to continue understanding the movement mechanisms, trying to comprehend more about not only how the movement is controlled and

when it is going to happen, but to also understand why is happens, including new variables and starting to understand the mechanisms of intercepting moving objects.

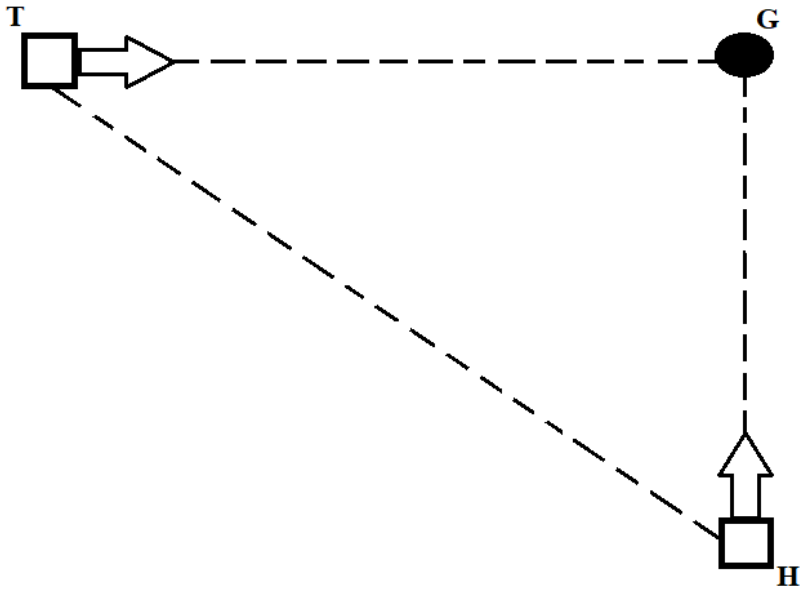

Figure 1 *- Visualization of tau-coupling during an interception task. The target (T) is moving towards target area (G), while the effector (H) is also moving towards the target area to intercept the moving target, while keeping the tau constant.*

Tau-coupling is a part of the general τ (tau) theory, proposed by David N. Lee, which suggests that the key figure in guiding movement is controlling the closure of gaps between effectors and their goals. By repeatedly sensing a single variable like time-to-closure at the current closure-rate, it is possible to achieve online guidance of gap closure, and that is called the τ of the gap or the tau variable (Lee et al., 2001). The τ_s of physical gaps can be detected via τ_s of sensory gaps between various sensory input arrays. By keeping the τ_s in a constant ratio between sensory element and target area, a guiding movement is being perceived, thus, tau-coupling should be predicted to be used to intercept a moving target (Lee, 2001a). Lee explains how to visualize tau-coupling in interception task with different acceleration speeds, where the tau of the target (T) and the movement of hand or effector (H) of target area (G) action gaps are kept constant and they have to close simultaneously (Figure 1) which means that the tau-effector (H) = K*tau-target (T) (Lee et al., 2001). This means that the K-value is a constant and it shows the

degree of control during a gap closure. Additionally, there are three ranges where K defines particular gap closing – if $0 < K \leq 0.5$, the movement is controlled and ends with soft contact. If $0.5 < K < 1$, the movement is less controlled and ends with a hard contact. In addition, if $K \geq 1$, the movement is portrayed by an absence of deceleration stage (Lee et al., 1999, Spencer et al., 2012). Previously done neuroimaging research with tau-coupling and a moving target shows that tau-coupling strategy is used to intercept a moving target during an interception task. (Postuma, 2019). Similar research with electroencephalography shows that sensorimotor area is directly associated with visual motion processing and execution of motor response (Engan, 2011) which are also important in understanding tau-coupling.

The current view on understanding how we perceive the surrounding world is based on two visual systems hypotheses, where visual information travels in two routes in the brain – a dorsal stream that affects the executive functions and the control of actions, and a ventral stream that helps us to identify objects (Van Polanen & Davare, 2015). Studies with physiological data show that the main areas in processing visual perception and radial motion are the medial temporal/visual area 5 (hMT/V5) (Dukelow, DeSouza & Culham et al., 2001; Smith, Wall, Williams & Singh, 2006). Brain activity during visual target interception tasks can be seen in the posterior parietal areas of the dorsal visual pathway (Delle Monache et al., 2017; Schenk et al., 2005) which is said to be responsible for guidance of interceptive actions (Dessing et al., 2013; Battaglia-Mayer et al., 2014). Processing of the sensorimotor information and motor execution is happening at the cortical motor areas of the brain (Lee et. Al., 2001b; Merchant et al., 2004). In general, dorsal and ventral streams are thought to improve and mature with age (Stiles, 2000), which can also be seen in previous research with the gradual shifting of neural oscillatory bands in the occipito-parietal brain region (Agyei et al., 2016).

Neuronal activity during interceptive tasks can be studied by electroencephalography (Tarantino et. al., 2014), where it can be found as visual evoked potentials (VEP's) and movement related potentials (MRP's). Visual evoked potentials and movement related potentials in visual perception tasks are captured by electroencephalography (EEG), due to its capabilities to detect neuronal events in high temporal resolution, in millisecond scale. EEG recordings of brain activity, even though limited to their spatial resolution when compared to other neuroimaging methods, are sufficient and detailed enough to show an accurate activity of

neuronal activity in the desired brain area. Previous research, using EEG to study VEP's and MRP's have proven to be valid as a meaning to study the motion perception both in adults and infants (van der Weel & van der Meer, 2009; Vilhelmsen et al., 2015). In similar previous EEG studies, there have been findings of a visual-motion related N2 component of visual evoked potentials in the occipital and parietal areas that gains higher peak latency with faster visual motion speed (Vilhelmsen et al., 2015; 2018; Pitzalis et al., 2012). There have also been similar findings about the motor responses of the P300 component latency peak of motor evoked potentials in motor and parietal areas that are related to reaching (Bozzacchi et al., 2012; McDowell et al., 2002; Tarantino et al., 2014) and the use of joystick during an interception task (Engan et al., 2011).

In 2020, Vicente Raja proposed a unified theory to integrate neural and behavioural scales of analysis of cognitive phenomena, based on the concept of resonance on the foundation of radical embodiment (Raja, 2020), to better understand the mechanisms of the mind. As Raja suggests, we should not look at behavioural and neural scale as two contrasting concepts, where experimental psychology covers more behavioural scales and neuroscience looks at the brain activity, but rather as two different activities of one organism. This framework is aimed to adhere together the neural and behavioural scope, which have previously been looked at separately, in a way to study the cognitive activities of one organism at the same time. This way, it would be possible to integrate various models of cognition, perception, and action from both experimental psychology and neuroscience, but with a twist of ecological psychology.

To understand what Raja means by radical embodiment, we need to take a step back to try to understand cognition as a concept. The most predominant theory of cognitive science explains cognition as a batch of computational mechanisms that are working in tandem to fix problems and solve tasks by using a set of previously created internal representations, which are used to guide the locomotion (Kawato, 1999). Radical embodiment can be both perceived and understood from the ecological or the enactive approach. In one approach, it can be seen as the opposite of the previously described predominant cognitive paradigm, where it rejects the mechanisms and representations (Gibson 1979; Varela et al. 1991; Hutto & Myin 2013, as mentioned in Raja, 2020), or on other side it can be viewed as a series of dynamical systems and explanations that interact with the action, perception, and environment (Chemero 2009; Di Paolo

et al. 2017; van Gelder 1998; Walmsley 2008, as mentioned in Raja, 2020). Ecological theory suggests that the environment constrains our view of the world, but enactive approach views how the individuals view the world differently, relatively to their skills and previous experiences (Baggs et al., 2018). Even though the radical embodiment perspective has gained popularity in recent years, there is no unified framework that would explain and tie it together as a field, thus, Raja (2020) proposes a way to elegantly tie it all together.

Raja suggests applying a resonance-based framework to unify these theories, based on Gibson's ecological approach to visual perception (Gibson, 1979), where resonance is argued as a foundation for perception and an alternative to the processing of information (Raja, 2020). Typical way of explaining resonance would be to imagine an acoustic guitar on its back. By plucking one of the strings, the body of guitar resonates to the vibration of the plucked string and amplifies the sound of it. Based on the example of guitar, resonance is tied to two concepts – amplification and coupling. Amplification helps to distinguish the specific characteristics of the object, for example, the guitar sound is perceived as one because of the combination of string vibration and resonance in its body. The coupling aspect ties it all together, combining both the string and the body of guitar in one or two related frequencies. These characteristics of resonance are what inspired J.J. Gibson to start using resonance in ecological psychology and what inspired Raja for applying the resonance framework to brain research.

The suggested resonance framework can be applied to the coupling of the dynamics of behavioural scale and neural scale, where perceptual information affects the neural and behavioural dynamics. Previous research tied to this framework is seen in the works of David Lee, where a perceiver must avoid an approaching object, where the relevant perceptual information is a tau variable that depicts the perceiver's time to collision of the object in their visual perception system (Lee, 2009). Similar research with tau time-to-contact coupling in looming show that the perceptual information is integral in both dynamics (van der Weel, van der Meer, 2009), because the perceptual information is available when the participant interacts with the environment. By running a recursive linear regression analysis, they found a significant relation of the Tau-coupling of dynamics of both neural scale and environment scale.

In the present study, high-density EEG recording was applied to assess target movement trajectory, finger kinematics, and brain activity during an interception task. The purpose of the

study was to understand the neuronal processes in brain during interception tasks that involve a motor activity. It is important to understand the connection between motor activity and brain activity in adults in interception tasks, as it is a significant process in our daily lives, starting from basic hand-eye coordination tasks to more complex situations, such as walking across the sidewalk and unconsciously assessing the approaching car speeds, or driving the car and responding to unexpected obstacles. It is expected to see a tau-coupling strategy between brain activity and motor activity while intercepting the moving target, while keeping the time to closure of the action gaps between finger and target area, moving target to the target catching area, brain activity and finger, and brain activity to moving target, constant. Both VEP and MRP peak latency changes are expected to increase with the faster acceleration of the target motion in the visual cortex and motor cortex. This study is conducted as a follow up research on *Perception-brain-action coupling during an interception task* project by Eva M. J. L. Postuma, F. R. (Ruud) van der Weel, & Audrey L. H. van der Meer (Postuma, 2019), based on David Lee's *Guiding contact by coupling the taus of gaps* (Lee, 2001). By replicating Lee's experiment on Tau-coupling with a twist of deeper investigation of the resonance aspect of the movement relation to the brain, it is proposed that tau-coupling exists between visual perception, finger movements, and motor evoked potentials in an interceptive timing task.

Methods

Participants

17 adults, aged 21 to 27 with the mean age of 24, were recruited for this study from the Norwegian University of Science and Technology (NTNU). From all the participants, 12 adults (6 male, 6 female) provided good datasets for brain analyses and were included in the study. All the participants reported that they were right-handed and that they were full-term born.

Electroencephalography is a non-invasive technique and causes no known physical harm to participants. At the beginning of study, all the participants gave their written informed consent and were informed about their rights to stop the experiment or withdraw from the study at any given time point. The Norwegian Regional Ethics Committee and the Norwegian Data Services for the Social Sciences approved the study.

Experimental stimuli and paradigm

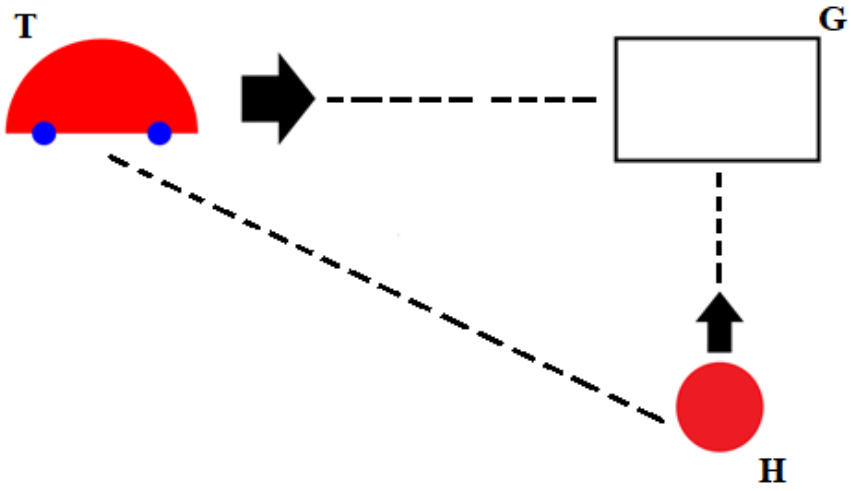

Figure 2 *- The experimental set-up where participants had to move up the red dot with their finger and intercept the horizontally moving car at the rectangular catching area. The car was moving under three accelerations of 0.12 m/s² (slow), 0.33 m/s² (medium), and 0.58 m/s² (fast), and the participant had to match their finger movement to the car acceleration in order for them to meet at the target area at the same time. The target (T) is moving towards target area (G),*

while the effector (H) is also moving towards the target area to intercept the moving target, while keeping the tau of the target to the target area and the tau of the effector to the target area, constant.

Software E-Prime 2.0 was used to display the experimental stimuli to a Windows Surface Hub touch screen with the size 1172 mm by 2203 mm, resolution of 2160 x 3840 pixels, operated by a HP Windows computer. The participants were seated on the edge of the chair approximately 70cm away of the screen as if on a high stool, so they would be able to comfortably reach the touchscreen, on which the target car, catching area, and dot were projected. Participants had to vertically move their finger on the touch screen to intercept a horizontally moving target car in a predetermined catching area. The size of the car was 57 mm by 35 mm, radius of the dot was 18 mm, and the size of the catching area rectangle was 59 mm by 42 mm, which are displayed in Figure 2. At the beginning of each trial, the distance between car and the rectangular catching area was 688 mm, while the distance from the dot to catching area was 660 mm. The car moved under three different accelerations that were randomly generated but never repeated in a row: 0.12 m/s² (slow), 0.33 m/s² (medium), or 0.58 m/s² (fast). Obtained car movement and finger movement coordinates were recorded in separate files for further analyses.

Data acquisition

EEG activity was recorded with a 256-channel Geodesic Sensor Net (GSN) 200 (Tucker, 1993) which was evenly distributed over the scalp. The net was connected to a high-input amplifier to ensure that the signals would reach maximum impedance set to 50 kΩ, as recommended for the optimal signal-to-noise ratio (Picton, 2001). EEG signals were then recorded with Net Station software at 500 Hz on a Macintosh computer, with applied online low-pass filter (200 Hz) and high-pass filter (0.1 Hz).

Different computers that were working in tandem coordinated the experimental process. HP computer with Windows 10 operating system that was built into the Microsoft Surface Hub displayed the experimental stimuli with the help of Python 3 software. The Python software

collected the additional experimental information data, such as trial information, trajectory data, finger movement trajectory coordinates, trial speed condition, and target hit or miss data. This information was saved into separate .txt files for offline data analyses.

Another HP computer with Windows XP operating system was responsible for E-Prime 2.0 Software and the coordination of the HP Windows 10 computer and Macintosh computer, so that all of the computers were working simultaneously during data collection.

Procedure

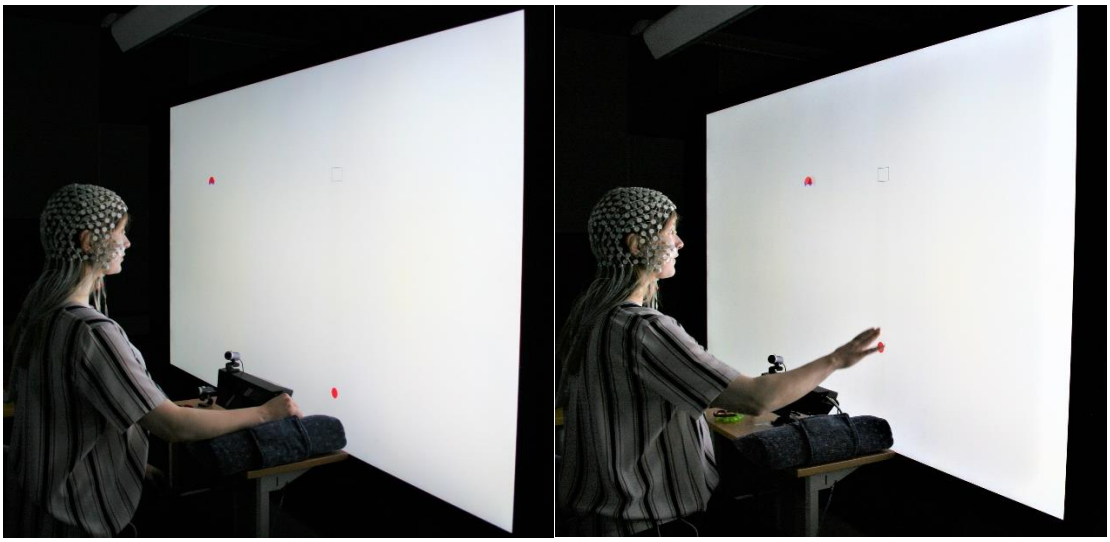

Figure 3 *- Experimental set up and procedure. Participants were sitting in front of a Windows Surface Hub touch screen and moving a red dot upwards with their finger to the designated catching area to intercept a horizontally moving car that was moving at different speeds, while wearing a 256-channel Geodesic Sensor Net.*

Participants arrived at the premises, received verbal information and instructions on the study, and signed the informed consent form. They were told that there would be a horizontally moving car from left to right on the screen and that they were to catch it in the designated target area by moving up a red dot with their finger vertically, until they would collide at the target area. Participants were instructed not to move their body or head, and only move their right arm and eyes to complete the task.

After listening to the experimental procedure instructions, the participant's head diameter was measured for the appropriate EEG net selection. The correct net was chosen and soaked in a saline electrolyte solution, partially dried, and placed on participant's head. After that, the participants were taken to the experimental room with the touch screen (Figure 3). Participants were asked to sit on the edge of the chair so that they would be comfortable in reaching the touchscreen and could move the arm freely. The EEG net was then connected to the amplifier. The participants were asked to remove any electronic devices that could disturb the EEG signal. All the assistants and spectators moved to the control room behind a glass window, leaving the participant alone in the experimental room, and checked the impedance of electrodes. If necessary, the impedance was corrected by either adjusting the position of the electrodes on the head or adding extra saline electrolyte solution. The experiment began when everything was checked and proved to be working as it was intended to do.

At the beginning of the experiment, participants performed six practice trials, two at each speed, to familiarize themselves with the experimental set-up and procedure. Every trial was defined as either a hit or a miss. The car started moving when the participants touched the dot on the screen with their right index finger. Between trials, the participants were allowed to rest their arm on a small pillow that was placed on the chair.

Once the practice trials were completed, the participants were told that the experiment would begin and that they should continue the experiment the same way. The experiment consisted of a total of 75 trials, which included a randomized order of 25 blocks that each included three trials of each speed condition. In this way, all trials were randomized but it also made sure that a condition would appear no more than twice in a row. Each experimental session took around 8 minutes, and only trials that were marked as hits were used in the data analyses. The average number of accepted hits were 18.1 for slow, 19.8 for medium, and 18.2 for fast speed. The number of bad electrodes that were excluded from the EEG data never exceeded 10% of the total count of 256, with the average of 5% bad electrodes for all participants together.

Data analysis

Behavioral data acquisition and analyses

Finger movement y-coordinates were extracted with Python 3 software at 100 Hz, according to the capabilities of the touch screen. For comparison with brain data that was acquired at 500 Hz, the finger movement data were linearly interpolated in Matlab from 100 Hz to 500 Hz by calculating the average distance between two following data points to match the frequencies at the same time period.

Time-series of car movement x-coordinates at three different constant accelerations were generated at 500 Hz and 100 Hz to allow for comparison with brain data and finger movement, respectively.

Brain data acquisition, analyses, and artefact removal

EEG recordings were segmented by NetStation software and transferred to an external server for analysis purposes. Data analyses were performed with the Brain Electrical Source Analysis (BESA) software. Averaging epoch was from -300 ms to 500 ms with a baseline definition of -100 ms to 0 ms with respect to stimulus onset. A notch filter was set to 50 Hz for line interference removal. Then data was high-pass filtered at 60 Hz and the low-pass filtered at 1.6 Hz. Channels were interpolated to the 81 standard electrodes of the 10-10 system for further analysis. Channels that were corrupted by artefacts and epochs from head or body movements were excluded from analyses or interpolated. If subjects had more than 10% of channels that were defined as bad, they were excluded from the present study.

VEP and MRP peak analysis and tau-coupling

Individual data of the slow, medium and fast speed conditions were averaged and combined into standardized 81-electrode configuration of the 10-10 International system. Brain wave latency peaks were selected for each participant for all three speeds, based on the theory that after every stimulus, there should be both a N200 and P300 response. Wherever possible, peaks were selected accordingly around 200-350 ms after the car started moving for N200 (Folstein, 2008) and 250-500 ms for P300 (Polich, 2007). Each participant had three latency

values for slow, medium, and fast speeds for visual evoked potential (VEP) and movement related potential (MRP). For each participant, the electrode with the highest latency peak quality and the most distinctive brain wave at approximate N200 and P300 component peaks were selected, keeping as close to the head midline as possible. Together for all participants, for VEPs the selected electrodes were O1, POz, PO4, and O2, while electrodes Cz, FCz, and FC2 were used for MRPs. The data was filtered using Gaussian sigma 3 filter for brainwaves and car movement and with Gaussian sigma 3 filter where the finger movement was involved.

Results

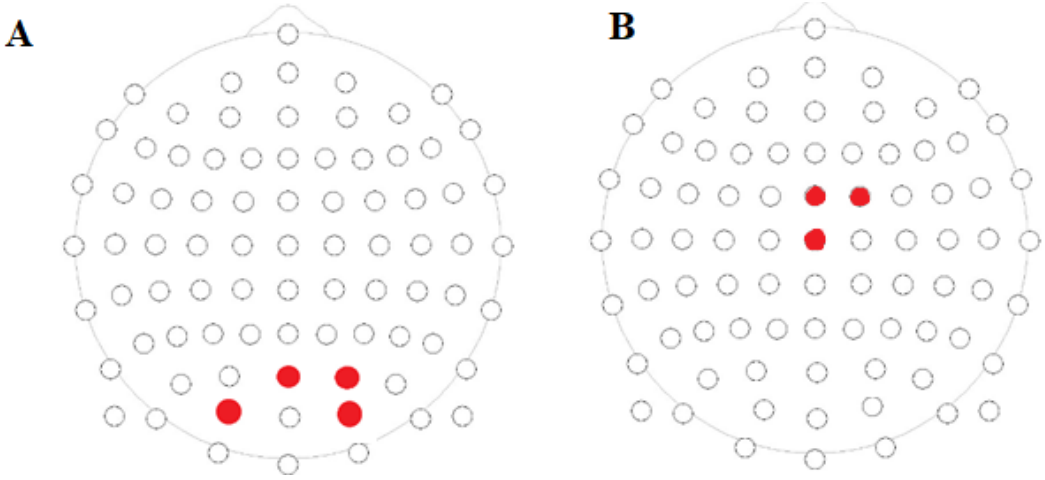

Figure 4 *- Human head model with nose facing north. Scalp localisation of the 81 standard electrodes with the selected electrodes are presented with red circles. The electrodes used in the study for VEP analyses in Figure 4A, from left to right and top to bottom: O1, POz, PO4, O2, and in Figure 4B for MRP analyses, from left to right and top to bottom: FCz, Cz and FC2.*

Visual evoked potential responses and analysis

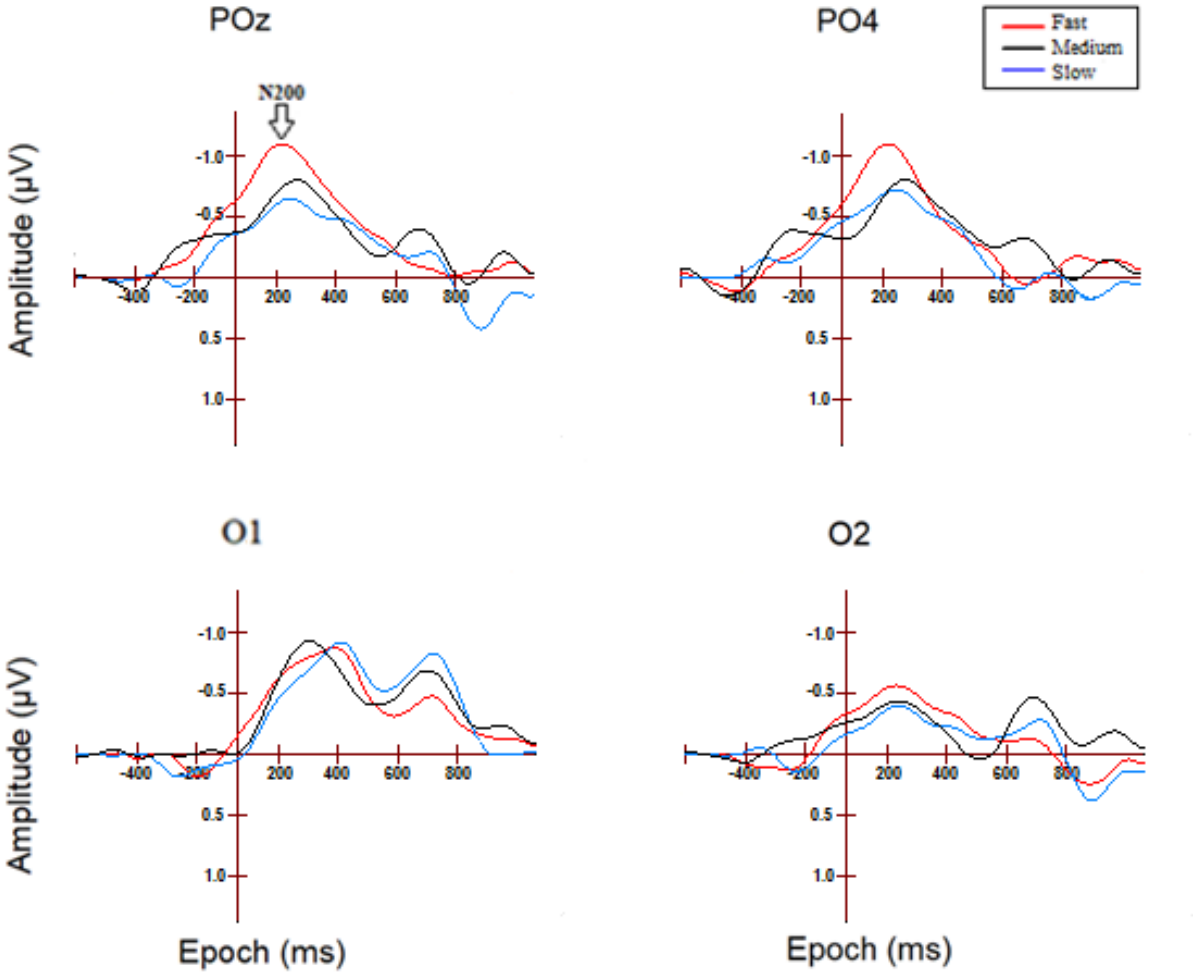

Figure 5 *- Grand-averaged waveforms of the VEP's for three speed conditions – fast, medium and slow in adults, with epoch ranging from -300 to 500ms. The arrow on the top left graph displays the N200 component of three different speeds – slow, medium, and fast. Epoch (ms) on X-axis, amplitude (uV) on Y-axis for displaying VEPs.*

To test for differences in N200 group latencies, a repeated measure ANOVA was performed with speed (slow, medium, fast) as within factors. In total, four grand averaged channels were selected for visual evoked potential response analysis, based on having the highest mean N200 amplitude – O1, POz, PO4, and O2, see Figure 4, and were selected as close as

possible to the midline of the brain. Figure 5 is displaying the grand average VEP waveforms of the four selected electrodes. The average mean N200 latency for the three speeds – slow, medium, and fast was 220 ms (SD=45), 260 ms (SD=49), and 301 ms (SD=52), as seen in Figure 6. A repeated measures ANOVA showed a main effect of target speed, F (2, 22) = 15.7, p < 0.0005, indicating that N2 latencies for motion increased significantly with the speed of the moving object.

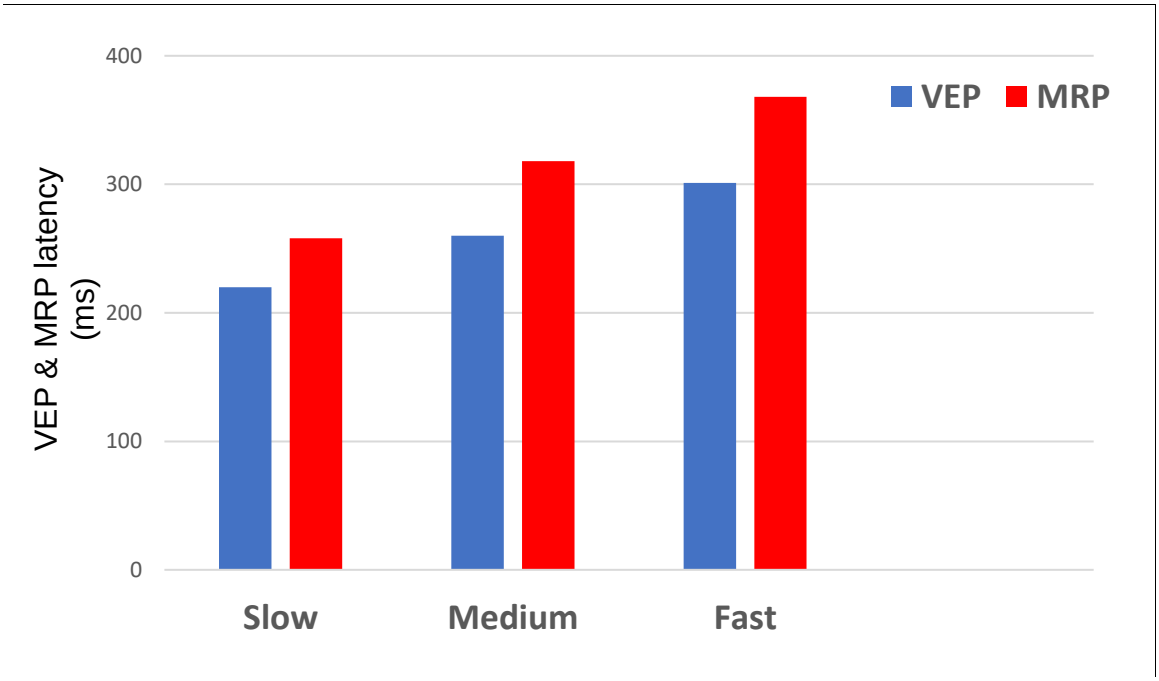

Figure 6 – *Average group mean differences in N200 and P300 peak latencies for VEP and MRP three different speed conditions – slow, medium, and fast. In all speed conditions, there is a statistically significant sequential difference in average peak latencies where the average peak latency increases with the increase of the speed of the moving object. The average MRP latency peak always is higher than the average VEP latency peak, showing a main effect between MRP and VEP latency peaks.*

Motor-related potential responses and analysis

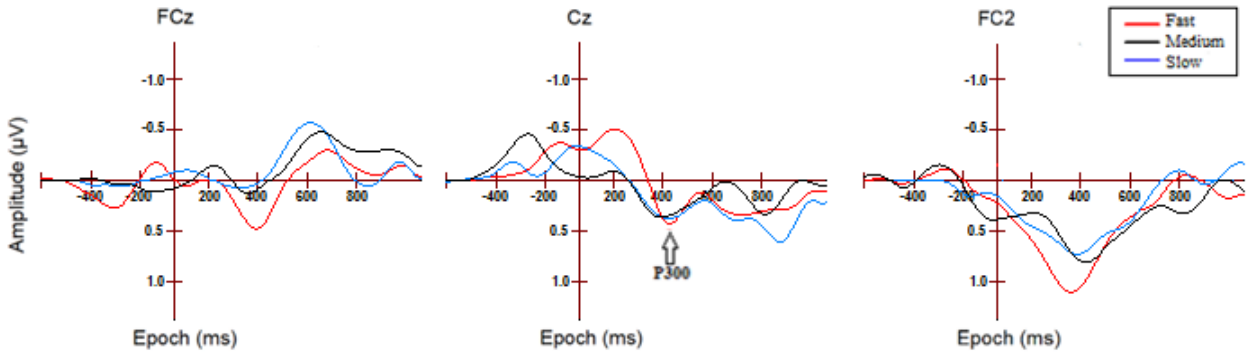

Figure 7 *- Grand-averaged waveforms of the MRP's for three speed conditions – fast, medium and slow in adults, with epoch ranging from -300 to 500ms. The arrow on the middle graph displays the P300 component of three different speeds – slow, medium, and fast. Epoch (ms) on X-axis, amplitude (uV) on Y-axis for displaying MRP's.*

To test for differences in P300 group latencies, a repeated measure ANOVA was performed with speed (slow, medium, fast) as within factors. In total, three grand averaged channels were selected for motor related potential response analysis, based on having the highest mean P300 amplitude – FCz, Cz and FC2, see Figure 4, and were selected as close as possible to the midline of the brain. Figure 7 is displaying the grand average MRP waveforms of the four selected electrodes. The average mean P300 latency for the three MRP speed conditions – slow, medium, and fast was 258 ms (SD=52), 318 ms (SD=69) and 368 ms (SD=81), as seen in Figure 6. A repeated measures ANOVA showed a main effect of target speed, F (2, 22) = 14.716, p < 0.0005, indicating that P300 latencies for motion increased significantly with the speed of the moving object.

Tau-coupling results

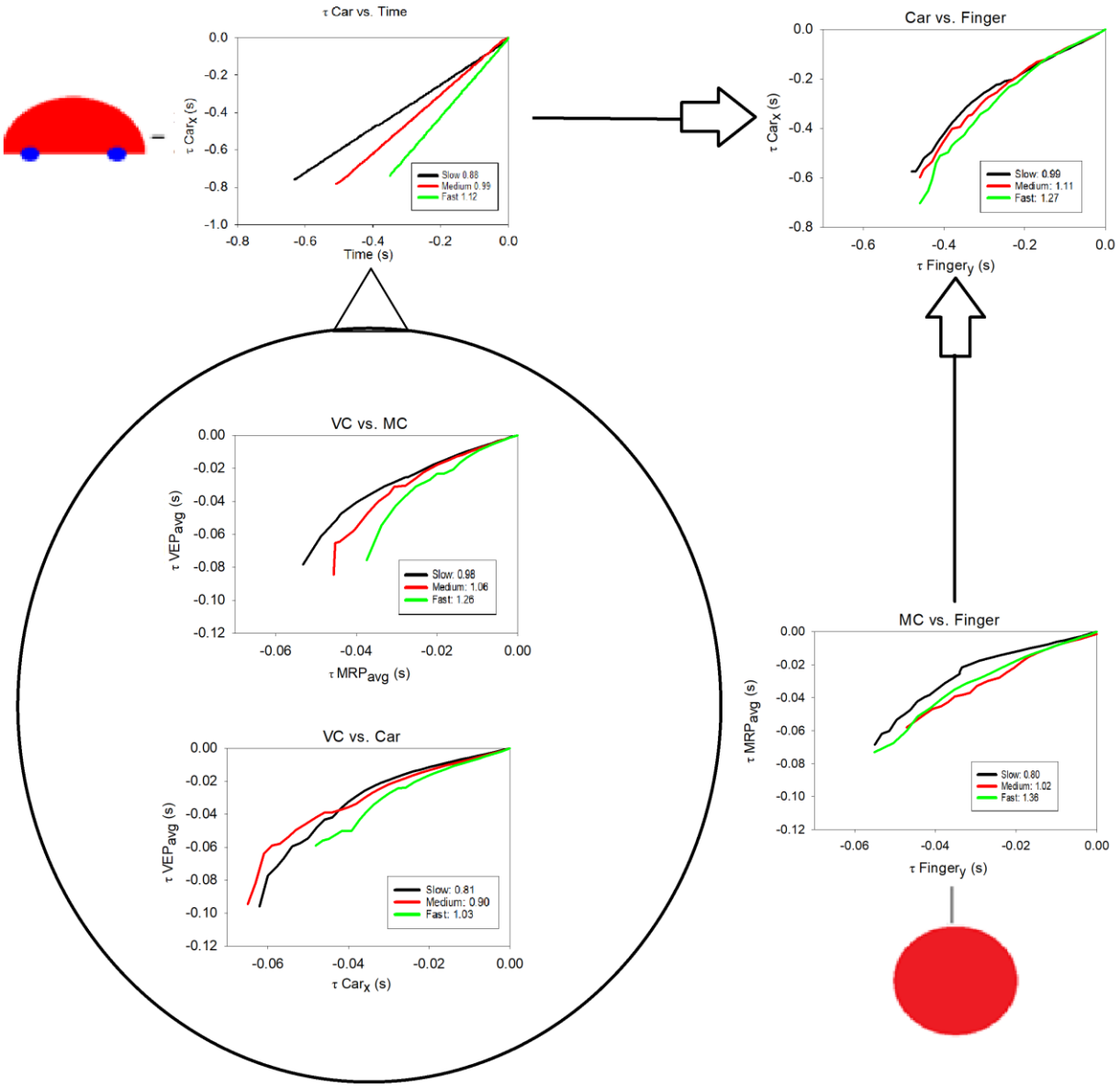

Figure 8 *- Tau-coupling results, depicting five different averaged tau-coupling graphs on a head model (nose up), that are thought to describe the technical and neural process of the interception task. From left to right and bottom to top, the graphs display tau of the car against time to collision, the car movement and finger movement tau-coupling, the visual cortex and motor cortex tau-coupling, the visual cortex and car movement tau-coupling and the motor cortex and finger movement tau-coupling. Each of the graphs display an average slope height for each tau-*

coupling to show the difference between three different speeds – slow, medium, and fast, and how it changes in each interaction.

		Finger movement					
		MRP			VEP		
		Slow (SD)	*Medium (SD)*	*Fast (SD)*	*Slow (SD)*	*Medium (SD)*	*Fast (SD)*
Brain activity	Index	4.00 (3.13)	3.17 (2.85)	2.58 (1.83)	1.91 (2.46)	1.25 (2.05)	3.41 (2.74)
	Slope	0.80 (0.15)	1.02 (0.31)	1.36 (0.39)	0.87 (0.09)	0.96 (0.45)	1.24 (0.42)
	R2	0.96 (0.01)	0.96 (0.01)	0.96 (0.01)	0.96 (0.01)	0.97 (0.02)	0.97 (0.01)
	% of Total	86.21 (10.70)	88.68 (10.23)	89.45 (7.57)	92.24 (9.87)	95.19 (7.71)	87.32 (9.50)
		Car movement					
		MRP			**VEP**		
		Slow (SD)	*Medium (SD)*	*Fast (SD)*	*Slow (SD)*	*Medium (SD)*	*Fast (SD)*
Brain activity	Index	5.08 (2.81)	4.08 (2.71)	5.41 (2.15)	4.25 (2.56)	2.83 (2.86)	4.25 (2.77)
	Slope	0.85 (0.06)	0.97 (0.12)	1.07 (0.07)	0.81 (0.09)	0.90 (0.13)	1.05 (0.13)
	R^2	0.96 (0.01)	0.96 (0.01)	0.96 (0.01)	0.96 (0.01)	0.96 (0.01)	0.96 (0.01)
	% of Total	83.04 (9.65)	85.01 (9.42)	79.58 (6.91)	84.20 (9.74)	89.90 (9.93)	84.66 (9.90)
		Brain activity (VEP)					
		Slow (SD)		*Medium (SD)*		*Fast (SD)*	
Brain activity (MRP)	Index	1.17 (1.8)		1.08 (1.98)		2.00 (2.66)	
	Slope	0.98 (0.14)		1.06 (0.16)		1.27 (0.17)	
	R^2	0.98 (0.02)		0.98 (0.02)		0.98 (0.02)	
	% of Total	94.36 (9.17)		95.69 (8.43)		91.10 (10.90)	
		Finger movement					
		Slow (SD)		*Medium (SD)*		*Fast (SD)*	
Car movement	Index	2.67 (2.83)		1.41 (2.23)		0.83 (1.95)	
	Slope	0.99 (0.07)		1.11 (0.09)		1.27 (0.09)	
	R^2	0.96 (0.01)		0.96 (0.01)		0.97 (0.01)	
	% of Total	94.52 (6.02)		96.74 (5.38)		97.99 (4.71)	

Figure 9 – *Average tau-coupling results, depicting tau-couplings between brain activity, finger movement and car movement. Each coupling includes either the coupling between two variables or with the differentiation between MRP and VEP when the couple includes brain activity, to see how the different brain regions react to the same stimuli. Each coupling includes average scores of index value, slope, percentage of total trials included and rate of* R^2.

Tau-coupling between car motion and finger movement coordinates

Tau-coupling analysis was conducted between car motion and finger movement coordinates for the three car speeds. A repeated measures ANOVA showed a significant difference between car motion and finger movement coordinates in three different speed conditions – slow, medium, and fast ($F(2, 22) = 52.854$, $p < 0.0005$). The average % of total included trials for the coupling were over 95% in all of the speed conditions, and the average R^2 was more than 96% in all of the speed conditions, as seen in Figure 9. The average tau slopes for slow, medium, and fast speed between both car motion and finger movement coordinates were 0.992 (SD=0.074), 1.114 (SD=0.095), and 1.273 (SD=0.086). By further visual inspection, it was possible to see a trend where the slopes gradually increased from flatter to steeper in slow, medium and fast speed conditions in 12 out of 12 participants, as seen in Attachments, Table 1. The averaged tau-coupling graphs for individual participants between car movement and finger movement can be found in the Attachments, Figure 5-17.

Tau-coupling between tau of the car and average time-to-collision

Tau-coupling analysis was conducted between the tau of the car and time-to-collision for the three car speeds. The average % of total included trials for the coupling were over 96% in all of the speed conditions, and the average R^2 was more than 97% in all of the speed conditions. The average tau slopes for slow, medium and fast speed conditions between tau of the car and average time-to-collision were 0.884 (SD=0.067), 0.989 (SD=0.094), and 1.12 (SD=0.088).

Tau-coupling between brain activity and car movement coordinates

Tau-coupling was conducted between average VEP and MRP latency peaks and car movement coordinates in three different speeds, comparing each speed condition between brain activity and car movement coordinates. A repeated measures ANOVA showed a significant difference between brain activity and car movement coordinates in three different speed conditions – slow, medium and fast in VEP ($F(2, 22) = 17.165$, $p < 0.0005$) and MRP ($F(2, 22) = 9.919$, $p < 0.005$). The average % of total included trials for the coupling were over 80% in all of the speed conditions in VEP and over 84% in MRP, as seen in Figure 9. The average R^2 was more than 95% in all of the speed conditions in VEP and MRP. The average tau slopes for slow,

medium, and fast speed in VEP between brain activity and car movement coordinates were 0.85 (SD=0.062), 0.967 (SD=0.127), and 1.074 (SD=0.074), and 0.808 (SD=0.099), 0.905 (SD=0.131), and 1.038 (SD=0.131) for MRP, accordingly. By further visual inspection it was possible to see a sequence where the slopes gradually increased from flatter to steeper in slow, medium and fast speed conditions in 10 out of 12 participants for VEP, but they were always gradually increasing in slow to fast conditions in 12 out of 12 participants. For MRP, the slopes gradually increased from flatter to steeper in slow, medium and fast speed conditions in 9 out of 12 participants, but they were always gradually increasing in slow to fast conditions in 12 out of 12 participants, as seen in Attachments, Table 2. The averaged tau-coupling graphs for individual participants between car movement and brain activity can be found in the Attachments, Figure 5-17.

Tau-coupling between brain activity and finger movement coordinates

Tau-coupling was conducted between average VEP and MRP latency peaks and finger movement coordinates in three different speeds, comparing each speed condition between brain activity and finger movement coordinates. A repeated measures ANOVA showed a significant difference between brain activity and finger movement coordinates in three different speed conditions – slow, medium and fast in VEP ($F(2, 22) = 14.545$, $p < .0005$) and MRP ($F(2, 22) = 7.321$, $p < .005$). The average % of total included trials for the coupling were over 87% in all of the speed conditions in VEP and over 86% in MRP, as seen in Figure 9. The average R^2 was more than 96% in all of the speed conditions in VEP and more than 95% in MRP. The average tau slopes for slow, medium and fast speed conditions in VEP between brain activity and finger movement coordinates were 0.872 (SD=0.086), 0.963 (SD=0.453) and 1.238 (SD=0.419) and 0.809 (SD=0.145), 1.022 (SD=0.316) and 1.357 (SD=0.386) for MRP, accordingly. By further visual inspection it was possible to see a sequence where the slopes gradually increased from flatter to steeper in slow, medium and fast speed conditions in 6 out of 12 participants for VEP, but they were always gradually increasing in slow to fast conditions in 12 out of 12 participants. For MRP, the slopes increasingly grew from flatter to steeper in slow, medium and fast speed conditions in 12 out of 12 participants, as seen in Attachments, Table 3. The averaged tau-coupling graphs for individual participants between finger movement and brain activity can be found in the Attachments, Figure 5-17.

Tau-coupling between MRP & VEP average latency peaks

Tau-coupling was conducted between MRP and VEP average latency peaks in three different speeds, comparing each speed condition between MRP and VEP average latency peaks. A repeated measures ANOVA showed a significant difference between MRP and VEP average latency peaks in three different speed conditions – slow, medium and fast ($F(2, 22) = 16.516$, $p < .0005$). The average % of total included trials for the coupling were over 90% in all of the speed conditions, and the average R^2 was more than 97% in all of the speed conditions, as seen in Figure 9. The average tau slopes for slow, medium and fast speed conditions between VEP and MRP average latency peaks were 0.981 (SD=0.144), 1.064 (SD=0.163) and 1.269 (SD=0.172). By further visual inspection it was possible to see a sequence where the slopes gradually increased from flatter to steeper in slow, medium and fast speed conditions in 8 out of 12 participants, but they were always gradually increasing in slow to fast conditions in 12 out of 12 participants, as seen in Attachments, Table 4. The averaged tau-coupling graphs for individual participants between VEP and MRP average latency peaks can be found in the Attachments, Figure 5-17.

Discussion

The aim of this study was to assess target movement trajectory, finger trajectory and brain activity during an interception task and explore the relationship between all of the variables by using a tau-coupling strategy. The main goal and purpose of the study was to try to understand how the brain activates during interception tasks that involve a motor activity. The present study was conducted as a follow up research on *Perception-brain-action coupling during an interception task* project by Postuma, van der Weel, & van der Meer (2019), based on Lee's *Guiding contact by coupling the taus of gaps* (Lee, 2001). Participants were introduced to an interception task where they had to manipulate an effector dot towards a moving car and catch it in the designated target area, while their brain activity was monitored and recorded by EEG. VEP and MRP analyses were conducted to assess the difference between electrical brain responses in three different speed conditions in both visual and motor cortex. Tau-coupling strategy was applied and calculated to find out whether tau-coupling exists between visual perception, finger movements, and motor evoked potentials in an interceptive timing task.

Literature on VEP and MRP analyses with EEG, starting from the early development in infants show that our perception is vastly improved as we mature. VEP research on infants show that during the first 3-4 months they could not differentiate between the types of visual motion, but as they reached 11-12 months of age, their perception of motion conditions had improved and they showed decreased latencies in N200 (Agyei et al., 2016). Another view on brain structure importance in VEP latency could be that axon-myelinated white matter is important in working memory performance and possibly processing speed (Chevalier, 2015). In addition, myelin volume fraction increases with age, thus possibly indicating that faster visual motion processing may also happen due to higher myelination. Similarly, research on age effects on the P300 latency show that there is clear evidence that P300 latency is lower in the first few years in life (Polich, 1990) and then increases as we mature (Kuba et al., 2012). As all of the participants were young adults and all of them were self-reported not to be premature born, it is safe to presume that their VEP response latencies had reached highest potential for differentiating between speed conditions.

The VEP and MRP analyses showed that during the interception task, participants were showing statistically significant differences in their brain activity when differentiating between three speeds – slow, medium and fast. The average mean N200 latency for VEP speed conditions was 220 ms, 260 ms and 301 ms, which have previously demonstrated to be found in other studies at around 200-350 ms (Folstein, 2008). The average mean P300 latency for the three MRP speed conditions was 258 ms, 318 ms and 368 ms, which also ties to theory that P300 latency peaks are mostly found at 250-500 ms (Polich, 2007). The sequential difference between three speeds with a statistically significant difference at $p < .0005$ level in both brain regions that also ties to theory where should we look for VEP and MRP responses, was in line with previous research on brain activity during interception tasks (Pitzalis et al., 2012; Engan et al., 2011; Tarantino et al., 2014). Both VEP and MRP speed condition average latency peaks sequentially cover the whole diapason of previously discovered VEP and MRP latency peaks, which leads us to believe that the selected average latency peaks are correct and usable for further use of tau-coupling strategy. The main effect found between MRP and VEP latency peaks may show how the information is processed through our brain, and the sequential difference between three speeds follows the same way. Once the input gets received as a VEP, in a short span of milliseconds it fires up as a neuronal change within MRP zones, which leads to believe that it is possible to see how the processed information travels through the dorsal-ventral pathways.

The results in this current study for tau-coupling between brain activity in visual cortex, motor cortex, car movement, and time-to-collision and finger movement lead to some interesting results, showing statistically significant correlation between all of the speed conditions. These results lead us to believe how our motor and visual cortex process visual and motion information, how it passes through the dorsal-ventral stream and automatically differentiates between slow, medium and fast speeds. The separate coupling between the tau of the car and time-to-collisions helps to understand the differences between speed conditions by creating a template of how the effector is moving throughout the different speeds and changing the slope of the coupling. As seen in the Figure 8, the slope steepness changes with the increase of the speed, displaying a main effect on the results, predicting that the faster the information flows, the steeper the tau-coupling slope is going to be. These results tightly go with Lee's research (2001), where he indicates that this differentiation between speeds can be explained by keeping the tau of the gap between effector and target coupled to the tau of the gap between the effector and the destination

zone (Lee, 1999). The study found a significant difference between slope variations in all of the cases, stating that as the speed gets faster, the slope of the tau also increases. The slope of tau represents a linear regression algorithm, placing all of the data points on a fitted line to find the correlation between two data sets, and how the increase of one variable effects the change of another. The higher steepness of faster speeds may represent a more difficult approach to processing the faster speeds in the brain, as well as the motor difficulties to move the effector to the target catching area. The strength of the tau-coupling r^2 in all of the cases was over 0.95 that is set by by the tau algorithm ($p<0.005$, t-test), which shows that the coupling is strong and believable. As previously mentioned, this work was closely written by following David Lee's life's work on tau-coupling and based on his principles, and it is possible to say that the results of this study relate to his research, showing how adults use a tau-coupling strategy to intercept moving objects (Lee et al., 2001). One difference between the previously found results and this experiment lies in the K values of the slope. It has been found out that the particular gap closing is being controlled with a K value which can the define the end of the movement with either soft or hard contact or the lack of deceleration stage (Lee et al., 1999; Spencer et al., 2012). The results in this study show that even though there was a statistically significant difference in the slope K values, it did not exactly tie to the previous research. It was thought that participants would control the effector and during the slow speed, they would use a soft contact strategy where the K value would be <0.5, but in all of the slow speed couplings, participants would have a K value of approximately 0.8-0.99, which shows a hard contact ($0.5\leq K<1$) strategy to control the target, based on its speed. For medium speed, the average K values were from 0.90 to 1.11 which shows how the adults used either hard ($0.5\leq K<1$) or non-controlled ($K\geq 1$) contact with the moving target, based on its speed. It could be possible that the used method was based on various individual settings and differences, such as previous life experiences, environmental settings or other. As all of the participants were approximately at the same age group, it should not have been a factor in K values, as it has been previously shown how differences in movement kinematics during an interception task depend on age (Kayed et al., 2009). And finally, the K values for fast movement speeds all showed a K value from 1.03 to 1.38 which shows how in the fastest speeds, participants mostly used a non-controlled ($K\geq 1$) contact strategy with the moving target. Another explanation for the difference between the findings of K value in this study and previous studies could be that the difference between speeds was not prominent enough for

contact strategies. Possibly, if the speed differences between slow, medium and fast speed conditions would have been broader, it would have been possible to see the soft contact strategy versus hard and non-controlled, but the difference in this study was strong enough to show differentiation in the brain activity.

As previously mentioned, this study was done as a follow up research and replication of the *Perception-brain-action coupling during an interception task* project by Postuma, van der Weel, and van der Meer (2019). Postuma and her colleagues conducted the research with exactly the same setting, protocol and methods, resulting in the same amount of trials per each speed condition. The averaged number hits for each condition were similar to this study - 18.1 for slow, 19.8 for medium, and 18.2 for fast, compared to 18.5 for slow, 20.3 for medium, and 17.6 for fast speed in Postuma's et al.'s (2019) study. In her study, she found out that the best electrodes with the highest N200 and P300 latencies and peak latency were POz, PO4, Oz, and O2 for the VEP analyses, and Cz, C2 and FCz for the MRP analyses, compared to, POz, PO4, O1 and O2 for VEP's, while electrodes Cz, FCz, and FC2 were used for MRP's. As seen, in both studies, most of the selected electrodes were the same; they were centered near the midline of the brain, where the dorsal and ventral stream would process the visual and movement information. The tau-coupling results in Postuma et al.'s (2019) study showed a statistically significant difference between three speed conditions in tau-coupling movement strategy with the car and finger movement ($p<0.001$), with the average peak latency differences in visual evoked potential responses ($p<0.005$), but no statistically significant difference between peak latency between three speed conditions in motor related potential responses ($p=0.717$). By replicating and adding more calculations to this study and choosing some other electrodes, it was possible to not only replicate the statistically significant results, but also improve them by finding new correlations between motor activity and brain activity. Postuma et al. (2019) used time-frequency analysis (TSE) to compare three speed conditions and did not find a difference between them. After combining them for easier analysis, she found desynchronized beta-oscillations in central areas, and desynchronized alpha-oscillations in both central and parietal areas, but no significant statistical correlations between any of the variables or brain activity. At the end of their paper, a suggestion for future studies was raised, where it was suggested to explore a direct relation between perceptual tau information, representation of tau in brain activity patterns and tau of

movement execution, and the present follow-up study has continued their suggestion, based on the framework they had built on before.

As it is possible to see, a lot of correlations between motor activity and brain activity show how they work in a tandem, just like Raja (2020) proposed in his unified theory for integrating neural and behavioural scales on the foundation of radical embodiment and Gibson's ecological approach to visual perception. So how does the resonance theory tie to this current study, is an interesting concept to think about. As mentioned previously, one of the most typical ways to understand resonance, would be by imagining a guitar laid on its back and by plucking one of the strings, which would then start a cascade of events, where the plucked string vibrates, resonates the body of the guitar and amplifies the sound. Therefore, this exact cascade of events is thought to also be seen in the proposed interception task. We propose that we can look at this interception task as a flow of information, as depicted in the graph in the results section, where it all starts at the target car which always travels in the same speed and direction, it is one variable that does not change for itself and stays constant all the time. Afterwards we start processing the information in our visual cortex and see the car standing at its start point, as well as we see the end catching area and the red dot that needs to be moved. If we look at the processing of the task from the traditional ways of explaining the perception and motor reactions as a fixed neural activity, we push the finger on top of the screen and see how it activates the car, it starts moving, and the visual cortex instantly communicates to the motor cortex, informing that there is a moving object and it needs to respond. Then the motor cortex activates the muscles of the arm and starts pushing the red dot towards the catching area, and finally when the car connects with the red dot, we see the correlation between the controlled arm movement and the constant movement of the car. If we think of the interception task in this way, we can apply the dorsal and ventral stream theory which would process the visual and movement information. Then we connect it with the tau theory and see the exact mathematical proof in statistically significant results of the perceived difference between three various speeds. From the resonance perspective, the organization of the neural activity could be seen as a dynamic and flexible assemblage of cascades. When looking at all of the tau-couplings and the main effect of speed on the steepness of slopes, it is possible to see the potential organization of information going from visual cortex to motor cortex, resonating throughout the brain, accordingly to perceived information of the stimuli. Once the visual information of the moving object, effector and the target area has been

received by the visual cortex, it can be passed over to other organizations where the information about the speed of the moving object and potential collision with the controlled dot, is processed with the exact time-to-collision information. Similar findings on combination of structural and functional organization in infant looming have been previously found by van der Meer and van der Weel (2019; 2009), where they proposed a two-fold principle of brain organisation. Firstly, following the retinotopic principles, structural, electrical activity makes its way through the retina to visual cortex, and then, secondly, after arriving at the visual cortex, the electrical activity spreads throughout various parts of visual cortex to principles of degenerate neural circuits (van der Weel et al., 2019). They continue explaining the resonance of the looming by comparing it to the fireworks, where once the rocket is shot up in the space, it explodes in various directions, comparing it to the dipole spread in looming trials. Similarly to their explanation, we can apply the same principles to the interception of a moving object, where the neuronal electrical activity spreads throughout the visual and motor cortex, activating and covering the area to successfully allow the distinction between the effector speeds and effectively calculate the actual time-to-collision. Another example mentioned by plucking the guitar string would be that the resonance of the brain activity during the interception task could be seen in two concepts – amplification and coupling. The moving car, effector dot and the designated target area are the individual amplifying stimuli that are tied together with the coupling, resonating together and creating a neuronal symphony. As seen in the methods section, all of the participants calculated time-to-collision and successfully registered a hit in more than 70% in all of the speed conditions, which shows how successfully the differentiation between speed conditions works. Wan der Weel & van der Meer found that even at a young age of 12-13 months, infants differentiated between various loom speeds with increasing values of the Tau-coupling constant for faster looms (Van der Weel & van der Meer, 2009), similarly how the K value changed in this study, thus, showing that these strategies are embedded even at a young age and continue perfecting throughout the lifetime.

Returning to the example that was given at the beginning by the last second play on the basketball court, it can be now discussed by everything that was found in this study. Our results show how the adult uses tau-coupling strategy during an interception task, which is done by controlling the action-gaps. During the last seconds of the inbound pass, we could now see the guiding of gaze, which results of closure of action-gaps between the motor activities, such as the

eyes and head movement to track the ball, feet and the ground to control movement and the arms and body to position for the interception. Everything that leads up to one moment, that could be externally seen as a simple motion by a spectator, could be viewed as a series of actions, processed in a bimodal fashion, combining the visual plus the articular action (Lee, 2009), resonating within our neural networks. In bimodal cases, the individual taus could be weighted and counted together, and then readjusted to accuracy. During our experiment, we gathered a series of individual taus which could be weighed together and compared by the motor and neuronal activities and their corresponding couplings with various speeds. It is possible to see how the change of speed affects the action-gaps in terms of steepness of the slopes, thus showing how the tau-coupling strategy is being used during an interception task, and we believe that the individual couplings are actually working all together in resonance to help in performing various tasks.

To sum it all up, the present study, the follow up it was based upon, and the extensive previous research that led to this point, show how adults successfully use a tau-coupling strategy for interception of moving objects. The current findings show how much is yet unknown about what is happening inside our minds unconsciously. The findings show that adults use a tau-coupling strategy to intercept a moving object and that the visual cortex and motor cortex works in tandem to do so, at the same time unconsciously differentiating between various speeds of the moving object. We believe that the results show how the perceptive information on moving objects is being communicated from parietal to motor areas, like in the two-stream information theory, but more in the sense of resonance that spreads the neuronal activity in surrounding brain areas. The results may prove beneficial not only for various fields of study but also for everyday situations where we do not even think about the unconscious processes that are happening in our brains. Unknowingly we use a tau-coupling strategy when we walk across the road and see the car approaching us, when someone throws a ball towards us or when we try to swat away an annoying fly that has been harassing us all evening. The results of this study could be helpful to continue research in sports science or military science, for example, in testing athletes or military personnel cognitive abilities in various settings. Future studies or similar follow up studies should include a broader range of participants for a more versatile comparison between groups, a different variety of speed conditions with larger spread of speed variations, a broader set of analyses, such as TSE analyses for analysing activities in the brain areas. In a grander scale, it

would be possible to conduct a longitudinal study in the development of infant visual and motor system by studying their brain activity patterns and movement execution in interception tasks and then replicate the experiment on the same participants years later to see how the visual and motor systems develop throughout the lifetime.

Reference list

Agyei, S. B., Van der Weel, F. R., & Van der Meer, A. L. (2016a). Longitudinal study of preterm and full-term infants: High-density EEG analyses of cortical activity in response to visual motion. Neuropsychologia, 84, 89-104. https://doi.org/10.1016/j.neuropsychologia.2016.02.001

Baggs, E., & Chemero, A. (2018). Radical embodiment in two directions. Synthese, 1-16 https://doi.org/10.1007/s11229-018-02020-9

Battaglia-Mayer, A., Buiatti, T., Caminiti, R., Ferraina, S., Lacquaniti, F., & Shallice, T. (2014). Correction and suppression of reaching movements in the cerebral cortex: Physiological and neuropsychological aspects. Neuroscience and Biobehavioral Reviews, 42, 232-251. http://dx.doi.org/10.1016/j.neubiorev.2014.03.002.

Bozzacchi, C., Giusti, M., Pitzalis, S., Spinelli, D., & Di Russo, F. (2012). Awareness affects motor planning for goal-oriented actions. Biological Psychology, 89 (2), 503-514. https://doi.org/10.1016/j.biopsycho.2011.12.020.

Brenner, E., & Smeets, J. B. J. (2018). Continuously updating one's predictions underlies successful interception. Journal of Neurophysiology, 120, 3257-3274.

Chevalier, N., Kurth, S., Doucette, M. R., Wiseheart, M., Deoni, S. C., Dean, D. C., 3rd, O'Muircheartaigh, J., Blackwell, K. A., Munakata, Y., & LeBourgeois, M. K. (2015). Myelination Is Associated with Processing Speed in Early Childhood: Preliminary Insights. PloS one, 10(10), e0139897. https://doi.org/10.1371/journal.pone.0139897

Delle Monache, S., Lacquaniti, F., & Gianfranco, B. (2017). Differential contributions to the interception of occluded ballistic trajectories by the temporoparietal junction, area hMT/V5+, and the intraparietal cortex. Journal of Neurophysiology, 118, 1809-1823. https://doi.org/10.1152/jn.00068.2017.

Dessing, J., Vesia, M., & Crawford, J. (2013). The role of areas MT+/V5 and SPOC in spatial and temporal control of manual interception: an rTMS study. Frontiers in Behavioral Neuroscience, 7, 1-15. https://doi.org/10.3389/fnbeh.2013.00015.

Dukelow, S. P., DeSouza, J. F., Culham, J. C.,van den Berg, A. V., Menon, R. S.,Vilis, T. (2001). Distinguishing subregions of the Human MT complex using visual fields and pursuit eye movements. Journal of Neurophysiology, 86, 1991–2000.

Engan, Ø., Van der Weel, F. R., & Van der Meer, A. L. H. (2011). Control of speed in the sensorimotor area during a visually guided joystick movement: A high-density EEG study. In E. P Charles and L. J. Smart (Eds.), Studies in Perception and Action XI (pp. 17-21). New York: Psychology Press.

M. J. L. Postuma, F. R. (Ruud) van der Weel, & Audrey L. H. van der Meer (2019). Perception-brain-action coupling during an interception task. Unpublished report, NTNU and Groningen University.

Folstein, J. R., & Van Petten, C. (2008). Influence of cognitive control and mismatch on the N2 component of the ERP: A review. Psychophysiology, 45, 152-170.

Gibson, J. J. (1958). Visually controlled locomotion and visual orientation in animals. The British Journal of Psychology, 49, 182–194. doi: 10.1111/j.2044-8295.1958.tb00656.x

Gibson, J. J. (1979). The Ecological Approach to Visual Perception. Boston, MA: Houghton Mifflin.

Kawato, M. (1999). Internal models for motor control and trajectory planning. Current Opinion in Neurobiology, 9, 718-727.

Kuba, M., Kremláček, J., Langrová, J., Kubová, Z., Szanyi, J., & Vít, F. (2012). Aging effect in pattern, motion and cognitive visual evoked potentials. Vision Research, 62, 9–16. https://doi.org/10.1016/j.visres.2012.03.014

Lee, D. N. (1976). A theory of visual control of braking based on information about time-to-collision. Perception, 5, 437–459. doi: 10.1068/p050437

Lee, D. N. (1998). Guiding movements by coupling taus. Ecological Psychology, 10, 221–250. doi: 10.1080/10407413.1998.9652683

Lee D. N. (2009). General Tau Theory: Evolution to date. Perception, 38(6), 837–850. https://doi.org/10.1068/pmklee

Lee, D. N., & Reddish, P. E. (1981). Plummeting gannets: a paradigm of ecological optics. Nature, 293, 293–294. doi: 10.1038/293293a0

Lee, D. N., Davies, M. N. O., Green, P. R., and Van Der Weel, F. R. (1993). Visual control of velocity of approach by pigeons when landing. Journal of Experimental Biology, 180, 85–104.

Lee, D. N., Georgopoulos, A. P., Clark, M. J. O., Craig, C. M., & Port, N. L. (2001a). Guiding contact by coupling the taus of gaps. Experimental Brain Research, 139, 151-159.

Lee, D. N., Lishman, J. R., and Thomson, J. A. (1982). Regulation of gait in long jumping. The Journal of Experimental Psychology: Human Perception and Performance, 8, 448–459. doi: 10.1037/0096-1523.8.3.448

Lee, D., Port, N., Kruse, W., & Georgopoulos, A. (2001b). Neuronal clusters in the primate motor cortex during interception of moving targets. Journal of Cognitive Neuroscience, 13(3), 319-331. https://doi.org/10.1162/08989290151137377.

McDowell, K., Jeka, J., Schöner, G., & Hatfield, B. (2002). Behavioral and electrocortical evidence of an interaction between probability and task metrics in movement preparation. Experimental Brain Research, 144(3), 303-313. https://doi.org/10.1007/s00221-002-1046-4.

Merchant, H., Battaglia-Mayer, A., & Georgopoulos, A. (2004). Neural responses in motor cortex and area 7a to real and apparent motion. Experimental Brain Research, 154(3), 291-307. https://doi.org/10.1007/s00221-003-1664-5.

Pitzalis, S., Strappini, F., de Gasperis, M., Bultrini, A., & Di Russo, F. (2013). Spatio-temporal brain mapping of motion-onset VEPs combined with fMRI and retinotopic maps. PLoS ONE, 7(4), e35771. https://doi.org/10.1371/journal.pone.0035771.

Polich, J. (2007). Updating P300: an integrative theory of P3a and P3b. Clinical Neurophysiology, 118(10), 2128–2148. https://doi.org/10.1016/j.clinph.2007.04.019

Polich, J., Ladish, C., & Burns, T. (1990). Normal variation of P300 in children: Age, memory span, and head size. The International Journal of Psychophysiology, 9(3), 237–248. https://doi.org/10.1016/0167-8760(90)90056-j

Raja, V. (2020). Resonance and radical embodiment. Synthese, 1-29. https://doi.org/10.1007/s11229-020-02610-6.

Rushton, S. K., Harris, J. M., Lloyd, M. R., & Wann, J. P. (1998). Guidance of locomotion on foot uses perceived target location rather than optic flow. Current Biology, 8, 1191–1194. doi: 10.1016/s0960-9822(07)00492-7

Schenk, T., Ellison, A., Rice, N., & Milner, A. (2005). The role of V5/MT+ in the control of catching movements: An rTMS study. Neuropsychologia, 43(2), 189-198. https://doi.org/10.1016/j.neuropsychologia.2004.11.006.

Smith, A.T., Wall, M.B., Williams, A. L., & Singh, K. D. (2006) .Sensitivity to optic flow in human cortical areas MT and MST. The European Journal of Neuroscience, 23,561–569.

Stiles J. (2000). Neural plasticity and cognitive development. Developmental neuropsychology, 18(2), 237–272. https://doi.org/10.1207/S15326942DN1802_5

Tarantino, V., De Sanctis, T., Straulino, E., Begliomini, C., & Castiello, U. (2014). Object size modulates fronto-parietal activity during reaching movements. European Journal of Neuroscience, 39(9), 1528-1537. 1 https://doi.org/0.1111/ejn.12512.

van Andel, S., McGuckian, T. B., Chalkley, D., Cole, M. H., & Pepping, G. J. (2019). Principles of the guidance of exploration for orientation and specification of action. Frontiers in Behavioral Neuroscience, 13, 231-232. https://doi.org/10.3389/fnbeh.2019.00231

van der Weel, F. R., & van der Meer, A. L. H. (2009). Seeing it coming: Infants' brain responses to looming danger. Naturwissenschaften, 96, 1385-1391.

van der Weel, F. R., Agyei, S. B., van der Meer, A. L. H. (2019). Infants' brain responses to looming danger: Degeneracy of Neural Connectivity Patterns. Ecological Psychology, 31(3), 182–197. https://doi.org/10.1080/10407413.2019.1615210

Van Polanen, V., & Davare, M. (2015). Interactions between dorsal and ventral streams for controlling skilled grasp. Neuropsychologia, 79(Pt B), 186–191. https://doi.org/10.1016/j.neuropsychologia.2015.07.010

Vilhelmsen, K., Agyei, S., van der Weel, F. R., & van der Meer, A. L. H. (2019). A high-density EEG study of differentiation between two speeds and directions of simulated optic flow in adults and infants. Psychophysiology, 56(1), e13281. https://doi.org/10.1111/psyp.13281.

Vilhelmsen, K., van der Weel, F. R., & van der Meer, A. L. H. (2015). A high-density EEG study of differences between three high speeds of simulated forward motion from optic flow in adult participants. Frontiers in Systems Neuroscience, 9, 146. https://doi.org/10.3389/fnsys.2015.00146.

Wolpert, D. M., Diedrichsen, J., & Flanagan, J. R. (2011). Principles of sensorimotor learning. Nature Reviews Neuroscience, 12, 739-751.

Attachments

Individual participant tau-coupling calculations

PARTICIPANT	VARIABLES	FINGER<>CAR MVMT			PARTICIPANT	VARIABLES	FINGER<>CAR MVMT		
		SLOW	MED	FAST			SLOW	MED	FAST
1	Start Index	4	4	0	7	Start Index	0	0	0
	Slope	0.9036	1.0756	1.2695		Slope	1.1153	1.1594	1.314
	R*2	0.9569	0.9542	0.9732		R*2	0.9851	0.9503	0.9596
	% of Total	93.1	91.49	100		% of Total	100	100	100
2	Start Index	6	3	0	8	Start Index	5	0	0
	Slope	0.9314	1.191	1.3098		Slope	0.9414	1.0332	1.1548
	R*2	0.9548	0.9504	0.9744		R*2	0.952	0.9537	0.9884
	% of Total	84.75	94	100		% of Total	89.8	100	100
3	Start Index	6	1	5	9	Start Index	6	7	0
	Slope	1.051	1.3305	1.4448		Slope	0.9208	0.9534	1.3422
	R*2	0.9521	0.9521	0.956		R*2	0.9523	0.9539	0.9647
	% of Total	88	97.37	89.13		% of Total	88.24	82.35	100
4	Start Index	0	0	0	10	Start Index	0	0	0
	Slope	1.0327	1.1166	1.2416		Slope	0.9492	1.0552	1.2086
	R*2	0.9877	0.9821	0.9863		R*2	0.979	0.9504	0.9606
	% of Total	100	100	100		% of Total	100	100	100
5	Start Index	0	0	5	11	Start Index	0	0	0
	Slope	1.0782	1.1513	1.2506		Slope	1.0413	1.1617	1.2819
	R*2	0.9683	0.9738	0.9516		R*2	0.9867	0.9682	0.9675
	% of Total	100	100	86.84		% of Total	100	100	100
6	Start Index	0	0	0	12	Start Index	5	2	0
	Slope	1.0366	1.0542	1.1255		Slope	0.9039	1.0805	1.3263
	R*2	0.9604	0.9831	0.9953		R*2	0.954	0.9506	0.9631
	% of Total	100	100	100		% of Total	90.38	95.65	100

Table 1 *– Individual participant tau-coupling results, depicting car movement and finger movement couplings for all 12 participants. Table describes individual participant tau-coupling scores for index value, slope, percentage of total trials included and rate of* R^2.

PARTICIPANT	VARIABLES	MRP			VEP		
		MRP SLOW	MRP MED	MRP FAST	VEP SLOW	VEP MED	VEP FAST
1	Start Index	7	7	7	0	4	7
	Slope	0.8151	0.9359	0.9615	0.9648	0.9925	1.0474
	R*2	0.9555	0.9514	0.9501	0.9601	0.9611	0.961
	% of Total	75.86	86.67	81.58	100	81.82	77
2	Start Index	0	5	7	6	0	0
	Slope	0.7807	0.8955	0.9719	0.9346	0.9583	0.9798
	R*2	0.9743	0.9503	0.9502	0.9519	0.9643	0.9861
	% of Total	100	80.77	75.86	77.97	100	100
3	Start Index	0	5	6	6	6	0
	Slope	0.892	0.8034	1.0561	0.8317	0.8872	0.9848
	R*2	0.9542	0.9532	0.9556	0.9532	0.9517	0.9772
	% of Total	100	81.48	77.73	75	81.82	100
4	Start Index	7	0	7	6	0	7
	Slope	0.8902	0.9207	1.2127	0.8557	0.9798	1.0504
	R*2	0.9504	0.964	0.9517	0.9578	0.9714	0.9574
	% of Total	75.76	100	77.14	75.19	100	80.37
5	Start Index	5	4	3	3	0	6
	Slope	0.8751	1.0403	1.108	0.6573	0.9727	1.1504
	R*2	0.9562	0.96	0.9608	0.9502	0.9586	0.9544
	% of Total	82.14	78.95	78.57	90.91	100	77.78
6	Start Index	2	6	4	1	0	0
	Slope	0.9186	1.0652	1.1361	0.8174	0.6346	0.8924
	R*2	0.9583	0.9571	0.9566	0.9532	0.9991	0.9785
	% of Total	95.83	76	80	95.83	100	100
7	Start Index	5	0	6	0	3	5
	Slope	0.8127	0.875	1.1086	0.7942	1.0159	1.037
	R*2	0.9585	0.9898	0.9612	0.9503	0.9504	0.9535
	% of Total	78.26	100	71.43	100	86.36	82,14
8	Start Index	7	7	0	6	7	3
	Slope	0.9299	0.9533	1.127	0.7301	0.8518	1.079
	R*2	0.9617	0.9548	0.9523	0.963	0.9615	0.9578
	% of Total	80.83	78.12	100	77.78	80	80
9	Start Index	7	6	7	5	2	6
	Slope	0.8742	0.9356	1.092	0.626	0.7639	1.3726
	R*2	0.9567	0.9515	0.9531	0.9537	0.9573	0.9536
	% of Total	75.53	77.78	78.08	80	93.75	80
10	Start Index	7	3	7	7	6	5
	Slope	0.7462	1.3071	1.0252	0.8129	1.1293	1.0204
	R*2	0.9585	0.9543	0.9572	0.962	0.9505	0.9617
	% of Total	78.79	78.57	76.67	75	80	79.17
11	Start Index	7	6	6	5	6	6
	Slope	0.7688	0.9481	1.0922	0.8565	0.8589	0.98
	R*2	0.9582	0.9522	0.9613	0.9538	0.9564	0.953
	% of Total	76.76	81.82	77.91	81.48	75	79.23
12	Start Index	7	0	5	6	0	6
	Slope	0.9048	0.9222	0.9999	0.8197	0.8137	0.8636
	R*2	0.9564	0.9563	0.9567	0.9559	0.9718	0.9603
	% of Total	76.76	100	80	81.25	100	77.78

Table 2 *- Individual participant tau-coupling results, depicting brain activity and car movement couplings for all 12 participants. Table describes individual participant tau-coupling scores for index value, slope, percentage of total trials included and rate of* R^2*, separated in MRP and VEP sections.*

PARTICIPANT	VARIABLES		MRP			VEP	
		MRP SLOW	MRP MED	MRP FAST	VEP SLOW	VEP MED	VEP FAST
1	Start Index	7	4	0	0	6	6
	Slope	0.7647	0.9122	1.0189	0.9329	0.972	1.0802
	R*2	0.9571	0.9518	0.953	0.957	0.9604	0.9532
	% of Total	75.07	86.21	100	100	77.78	76.92
2	Start Index	7	5	4	0	0	6
	Slope	0.8865	1.052	1.2196	0.9352	0.9741	1.5625
	R*2	0.954	0.9555	0.9602	0.9659	0.9541	0.9584
	% of Total	77.42	79.17	83.33	100	100	77.78
3	Start Index	0	0	4	3	0	0
	Slope	0.8514	0.8582	0.9934	0.8459	0.8114	1.0378
	R*2	0.9558	0.9518	0.958	0.9563	0.993	0.9998
	% of Total	100	100	82.61	86.36	100	100
4	Start Index	2	6	5	0	0	0
	Slope	0.8158	1.7796	1.8384	1.041	2.2748	2.4137
	R*2	0.9639	0.9505	0.9573	0.984	0.97	0.988
	% of Total	93.75	75.5	80.77	100	100	100
5	Start Index	7	5	3	0	0	1
	Slope	0.7598	0.7807	1.2845	0.7357	1.0322	1.1513
	R*2	0.9565	0.9611	0.9513	0.9691	0.9543	0.9648
	% of Total	75	78.26	88.46	100	100	96.97
6	Start Index	0	0	0	0	0	2
	Slope	0.8812	0.9293	1.5577	0.8366	0.6586	1.3452
	R*2	0.9648	0.9628	0.9853	0.9729	0.9986	0.9628
	% of Total	100	100	100	100	100	89.47
7	Start Index	1	0	4	0	2	4
	Slope	0.3884	0.6412	1.1769	0.7499	0.6372	0.9401
	R*2	0.9697	0.9963	0.9524	0.9873	0.959	0.9541
	% of Total	94.44	100	83.33	100	91.3	84.62
8	Start Index	7	0	0	5	0	3
	Slope	0.8175	1.5052	1.6972	0.8457	0.4618	0.9826
	R*2	0.9637	0.9703	0.9979	0.9574	0.9893	0.9671
	% of Total	75.22	100	100	81.48	100	78.57
9	Start Index	5	7	1	5	0	0
	Slope	0.8547	0.9775	1.0652	0.8785	0.9082	1.3702
	R*2	0.9539	0.9533	0.9633	0.9621	0.9839	0.9695
	% of Total	83.33	80.83	96.3	77.27	100	100
10	Start Index	5	7	3	6	4	7
	Slope	0.9035	1.0668	1.1993	0.9491	1.1365	0.9703
	R*2	0.9594	0.9523	0.9554	0.9558	0.9619	0.9621
	% of Total	84.37	77.17	88	77.78	85.19	83.01
11	Start Index	5	3	3	4	3	6
	Slope	0.8169	0.8919	2.2116	0.8163	0.8306	1.0619
	R*2	0.9565	0.9543	0.9585	0.9525	0.9604	0.9542
	% of Total	84.37	90.32	88	84	88	82.73
12	Start Index	7	1	4	0	0	6
	Slope	0.8997	0.8785	1.0286	0.897	0.8589	0.9424
	R*2	0.9632	0.9517	0.9557	0.9535	0.9956	0.9538
	% of Total	75.86	96.67	82.61	100	100	77.78

Table 3 *- Individual participant tau-coupling results, depicting brain activity and finger movement couplings for all 12 participants. Table describes individual participant tau-coupling scores for index value, slope, percentage of total trials included and rate of* R^2*, separated in MRP and VEP sections.*

PART.	VARIABLES	MRP<->VEP			PART.	VARIABLES	MRP<->VEP		
		SLOW	MED	FAST			SLOW	MED	FAST
1	Start Index	2	2	1	7	Start Index	4	0	0
	Slope	1.0136	1.381	1.2018		Slope	0.6062	0.7885	1.0569
	R*2	0.9602	0.9637	0.9555		R*2	0.961	0.9773	0.9956
	% of Total	92.86	95.83	96.15		% of Total	77.78	100	100
2	Start Index	0	0	0	8	Start Index	0	0	3
	Slope	0.8793	0.9046	0.9699		Slope	1.1171	1.0869	1.3044
	R*2	0.9976	0.9869	0.9986		R*2	0.9984	0.992	0.9734
	% of Total	100	100	100		% of Total	100	100	75
3	Start Index	4	1	7	9	Start Index	0	0	0
	Slope	0.9331	1.2612	1.2957		Slope	1.0114	1.0833	1.1527
	R*2	0.9624	0.9647	0.9607		R*2	0.9856	0.9929	0.9974
	% of Total	84.62	96.55	79.57		% of Total	100	100	100
4	Start Index	0	0	7	10	Start Index	0	4	0
	Slope	1.0906	1.1737	1.4117		Slope	0.9768	1.142	1.4534
	R*2	0.9979	0.9831	0.9675		R*2	0.996	0.9501	0.963
	% of Total	100	100	76.67		% of Total	100	78.95	100
5	Start Index	0	6	3	11	Start Index	0	0	0
	Slope	0.9562	0.9868	1.5456		Slope	1.0772	0.9572	1.4367
	R*2	0.9962	0.9516	0.962		R*2	0.9992	0.9907	0.998
	% of Total	100	76.92	76.92		% of Total	100	100	100
6	Start Index	0	0	3	12	Start Index	4	0	0
	Slope	1.1606	0.9463	1.2308		Slope	0.9519	1.0586	1.1675
	R*2	0.9876	0.9826	0.954		R*2	0.9617	0.9956	0.993
	% of Total	100	100	88.89		% of Total	77.07	100	100

Table 4 *– Individual participant tau-coupling results, depicting MRP and VEP couplings for all 12 participants. Table describes individual participant tau-coupling scores for index value, slope, percentage of total trials included and rate of* R^2.

Individual participant tau-coupling graphs

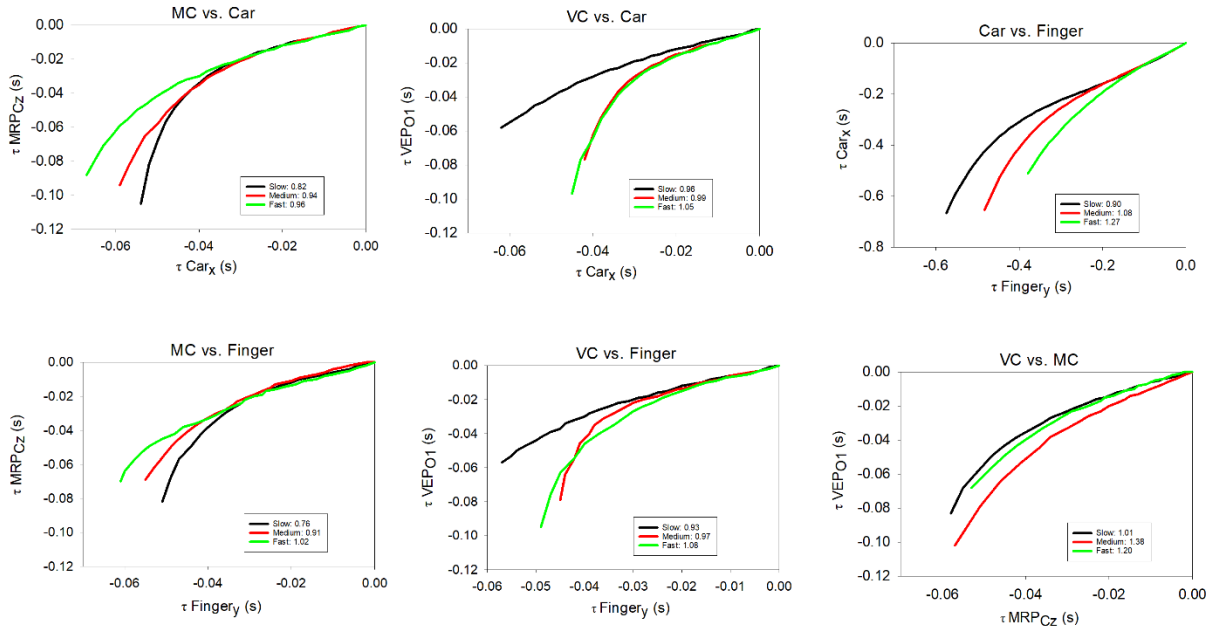

Figure 5 *– Participant 1 tau-coupling results, depicting six different tau-coupling graphs, that are thought to describe the technical and neural process of the interception task. From left to right and top to bottom, the graphs display the tau-coupling of the motor cortex and car movement, visual cortex and car movement, the car movement and finger movement, the motor cortex and finger movement, the visual cortex and finger movement, the visual cortex and motor cortex. All six graphs display an average slope height for each tau-coupling to show the difference between three different speeds – slow, medium, and fast, and how it changes in each interaction, with each coupling variable on X or Y axis.*

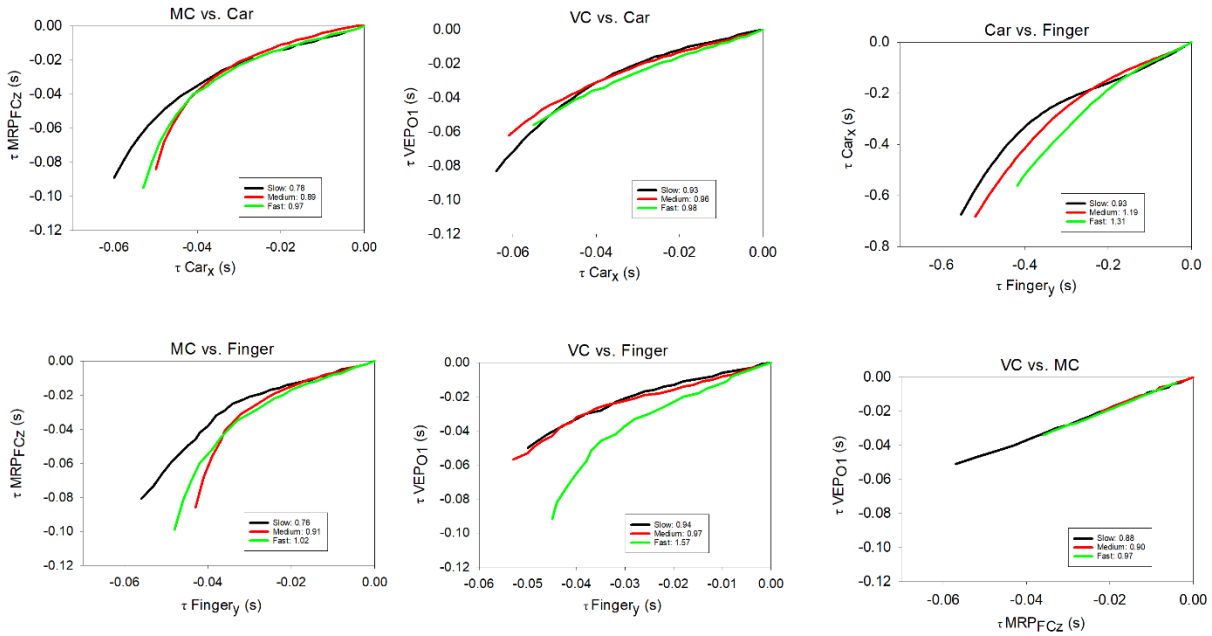

Figure 6 *– Participant 2 tau-coupling results, depicting six different tau-coupling graphs, that are thought to describe the technical and neural process of the interception task. From left to right and top to bottom, the graphs display the tau-coupling of the motor cortex and car movement, visual cortex and car movement, the car movement and finger movement, the motor cortex and finger movement, the visual cortex and finger movement, the visual cortex and motor cortex. All six graphs display an average slope height for each tau-coupling to show the difference between three different speeds – slow, medium, and fast, and how it changes in each interaction, with each coupling variable on X or Y axis.*

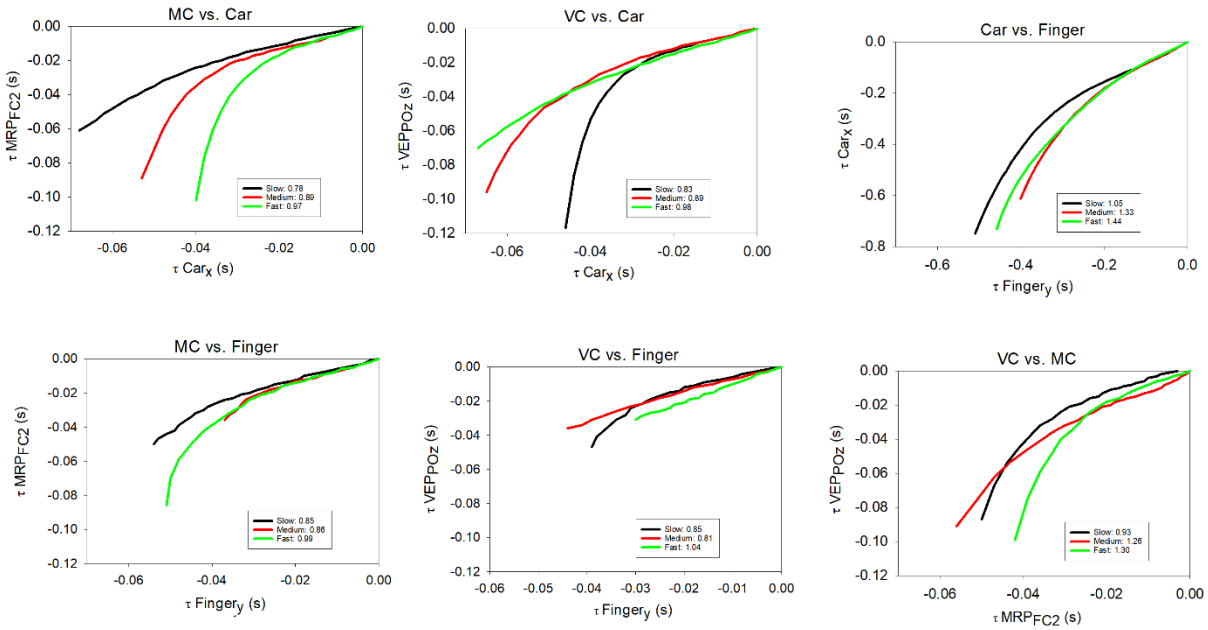

Figure 7 *– Participant 3 tau-coupling results, depicting six different tau-coupling graphs, that are thought to describe the technical and neural process of the interception task. From left to right and top to bottom, the graphs display the tau-coupling of the motor cortex and car movement, visual cortex and car movement, the car movement and finger movement, the motor cortex and finger movement, the visual cortex and finger movement, the visual cortex and motor cortex. All six graphs display an average slope height for each tau-coupling to show the difference between three different speeds – slow, medium, and fast, and how it changes in each interaction, with each coupling variable on X or Y axis.*

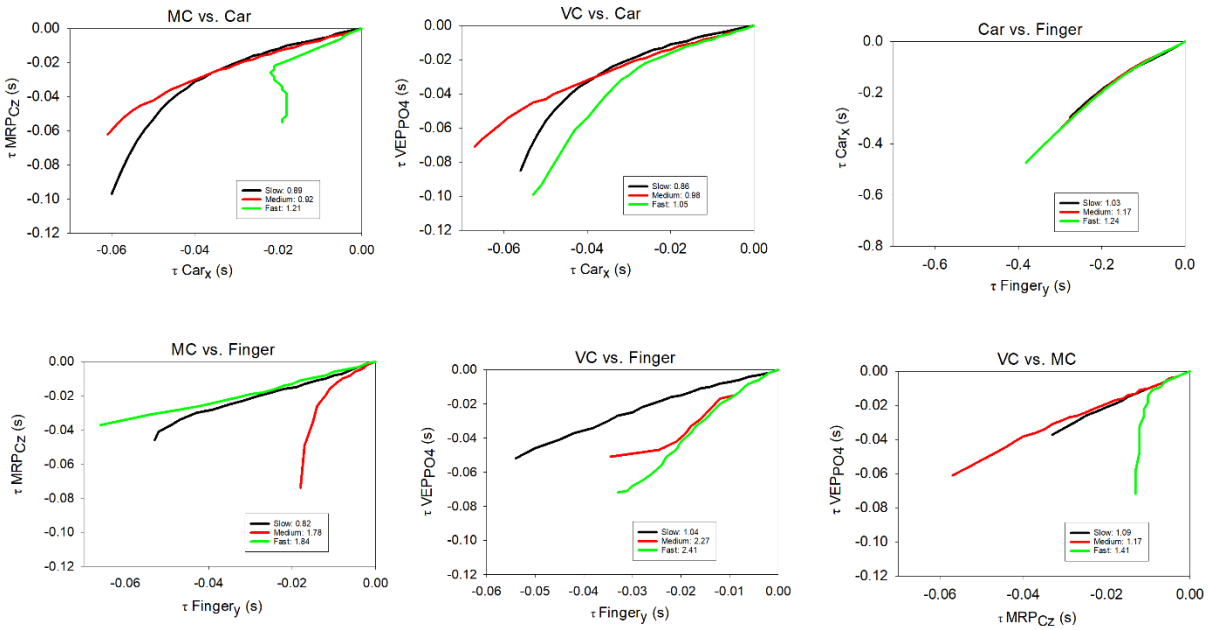

Figure 8 *– Participant 4 tau-coupling results, depicting six different tau-coupling graphs, that are thought to describe the technical and neural process of the interception task. From left to right and top to bottom, the graphs display the tau-coupling of the motor cortex and car movement, visual cortex and car movement, the car movement and finger movement, the motor cortex and finger movement, the visual cortex and finger movement, the visual cortex and motor cortex. All six graphs display an average slope height for each tau-coupling to show the difference between three different speeds – slow, medium, and fast, and how it changes in each interaction, with each coupling variable on X or Y axis.*

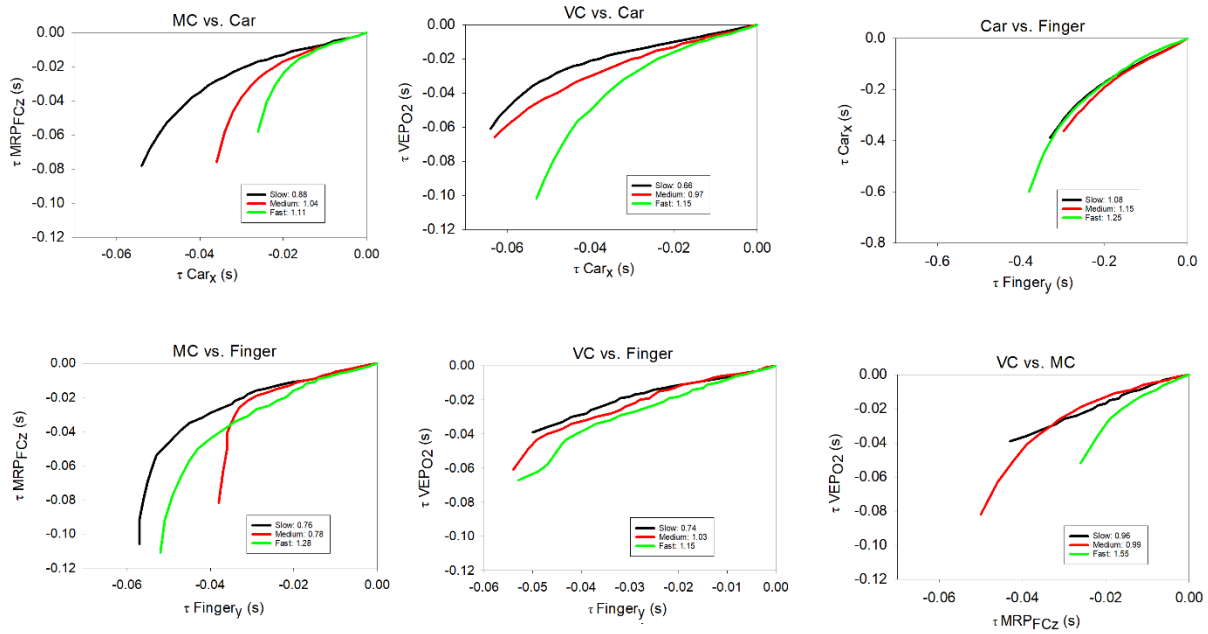

Figure 9 *– Participant 5 tau-coupling results, depicting six different tau-coupling graphs, that are thought to describe the technical and neural process of the interception task. From left to right and top to bottom, the graphs display the tau-coupling of the motor cortex and car movement, visual cortex and car movement, the car movement and finger movement, the motor cortex and finger movement, the visual cortex and finger movement, the visual cortex and motor cortex. All six graphs display an average slope height for each tau-coupling to show the difference between three different speeds – slow, medium, and fast, and how it changes in each interaction, with each coupling variable on X or Y axis.*

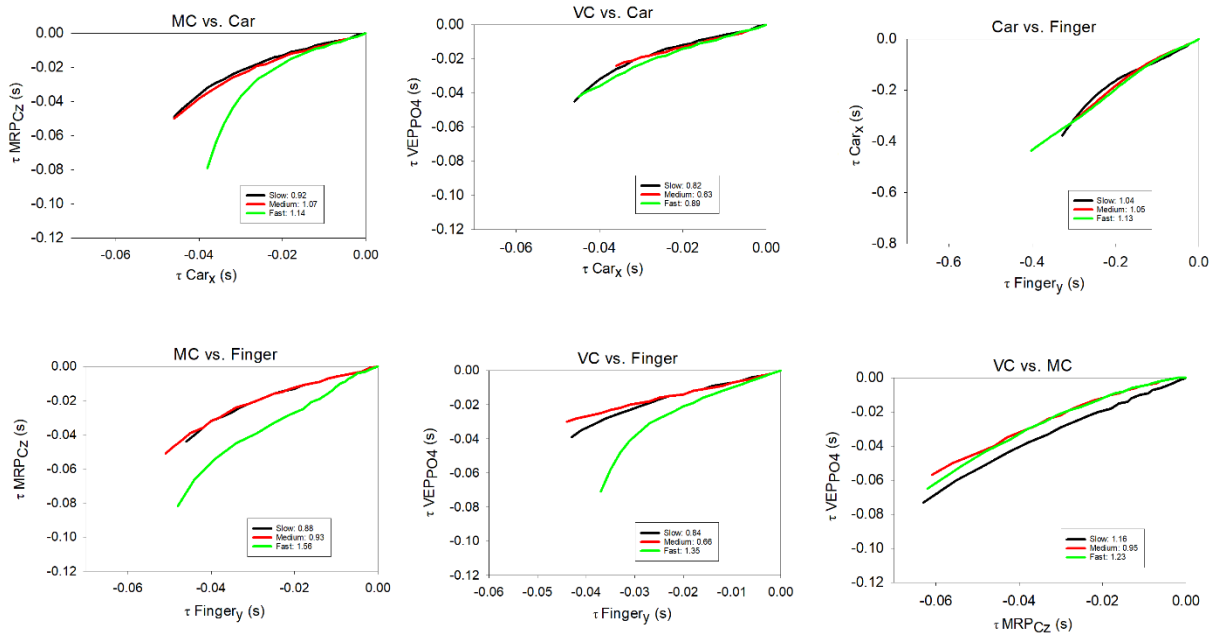

Figure 10 *– Participant 6 tau-coupling results, depicting six different tau-coupling graphs, that are thought to describe the technical and neural process of the interception task. From left to right and top to bottom, the graphs display the tau-coupling of the motor cortex and car movement, visual cortex and car movement, the car movement and finger movement, the motor cortex and finger movement, the visual cortex and finger movement, the visual cortex and motor cortex. All six graphs display an average slope height for each tau-coupling to show the difference between three different speeds – slow, medium, and fast, and how it changes in each interaction, with each coupling variable on X or Y axis.*

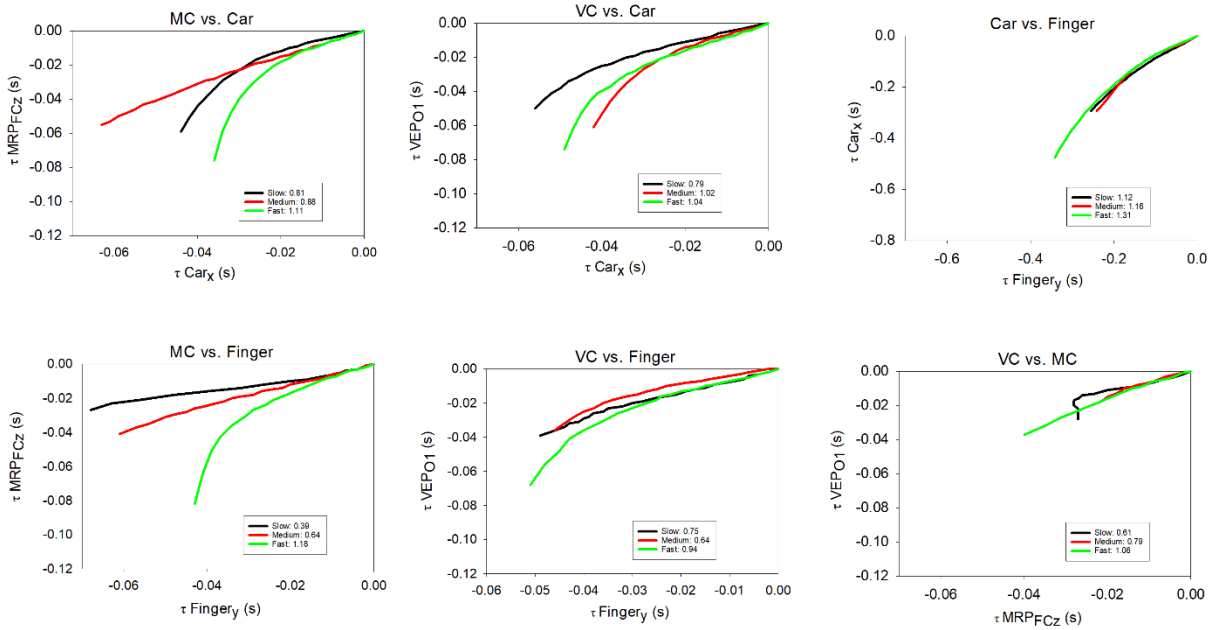

Figure 11 *– Participant 7 tau-coupling results, depicting six different tau-coupling graphs, that are thought to describe the technical and neural process of the interception task. From left to right and top to bottom, the graphs display the tau-coupling of the motor cortex and car movement, visual cortex and car movement, the car movement and finger movement, the motor cortex and finger movement, the visual cortex and finger movement, the visual cortex and motor cortex. All six graphs display an average slope height for each tau-coupling to show the difference between three different speeds – slow, medium, and fast, and how it changes in each interaction, with each coupling variable on X or Y axis.*

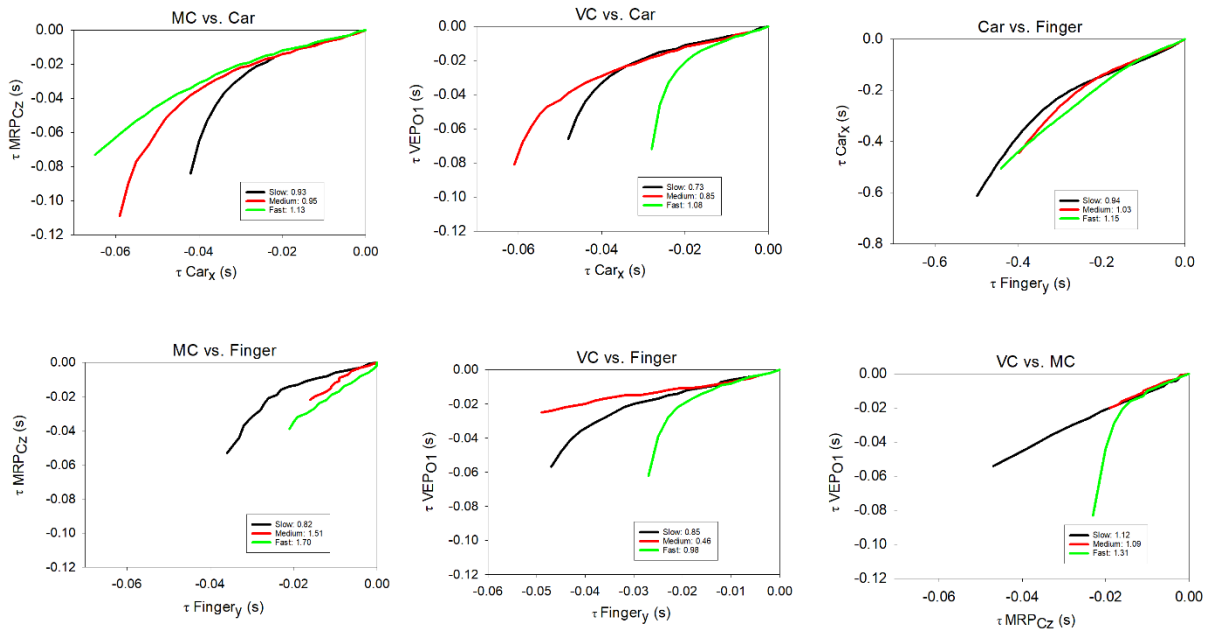

Figure 12 *– Participant 8 tau-coupling results, depicting six different tau-coupling graphs, that are thought to describe the technical and neural process of the interception task. From left to right and top to bottom, the graphs display the tau-coupling of the motor cortex and car movement, visual cortex and car movement, the car movement and finger movement, the motor cortex and finger movement, the visual cortex and finger movement, the visual cortex and motor cortex. All six graphs display an average slope height for each tau-coupling to show the difference between three different speeds – slow, medium, and fast, and how it changes in each interaction, with each coupling variable on X or Y axis.*

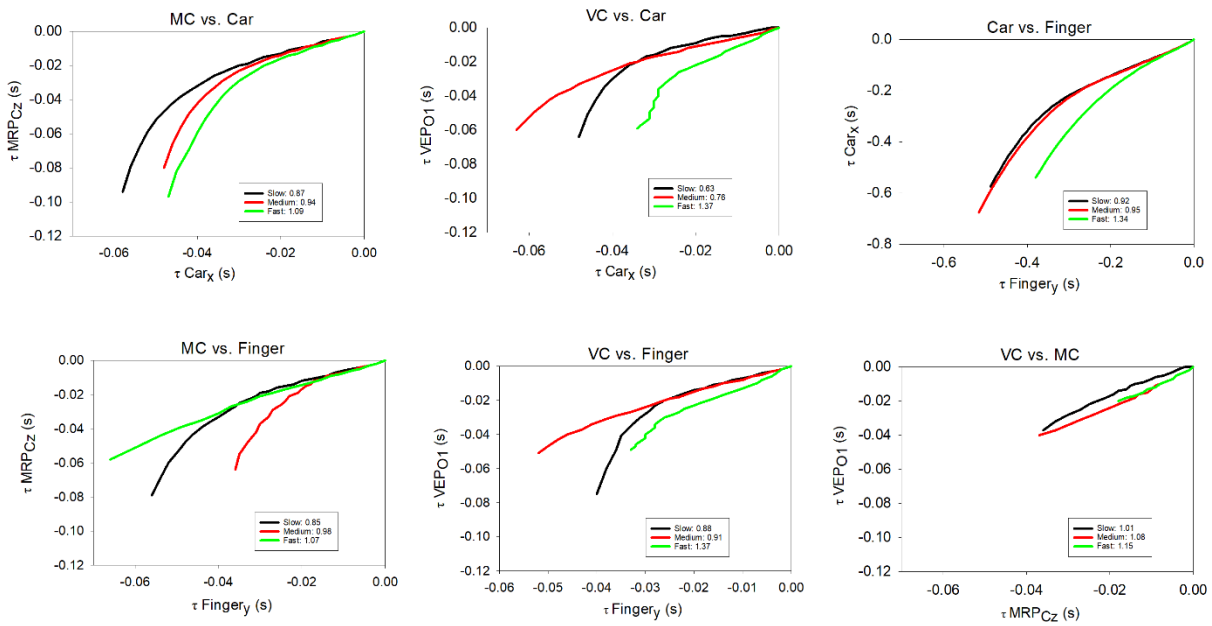

Figure 13 *– Participant 9 tau-coupling results, depicting six different tau-coupling graphs, that are thought to describe the technical and neural process of the interception task. From left to right and top to bottom, the graphs display the tau-coupling of the motor cortex and car movement, visual cortex and car movement, the car movement and finger movement, the motor cortex and finger movement, the visual cortex and finger movement, the visual cortex and motor cortex. All six graphs display an average slope height for each tau-coupling to show the difference between three different speeds – slow, medium, and fast, and how it changes in each interaction, with each coupling variable on X or Y axis.*

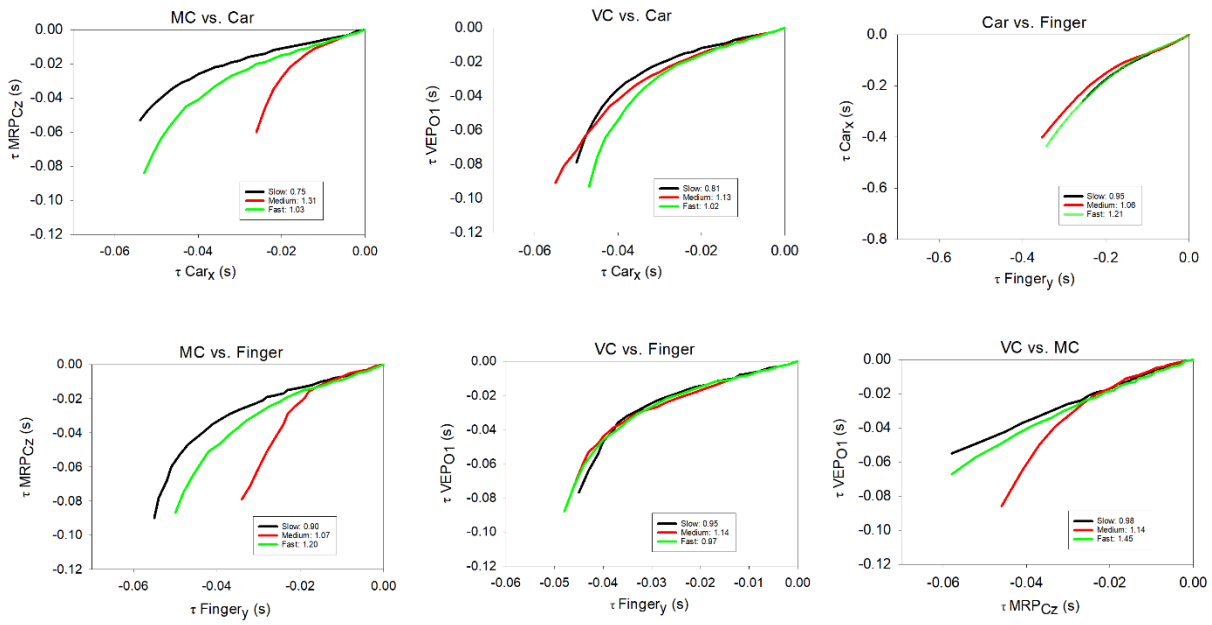

Figure 14 *– Participant 10 tau-coupling results, depicting six different tau-coupling graphs, that are thought to describe the technical and neural process of the interception task. From left to right and top to bottom, the graphs display the tau-coupling of the motor cortex and car movement, visual cortex and car movement, the car movement and finger movement, the motor cortex and finger movement, the visual cortex and finger movement, the visual cortex and motor cortex. All six graphs display an average slope height for each tau-coupling to show the difference between three different speeds – slow, medium, and fast, and how it changes in each interaction, with each coupling variable on X or Y axis.*

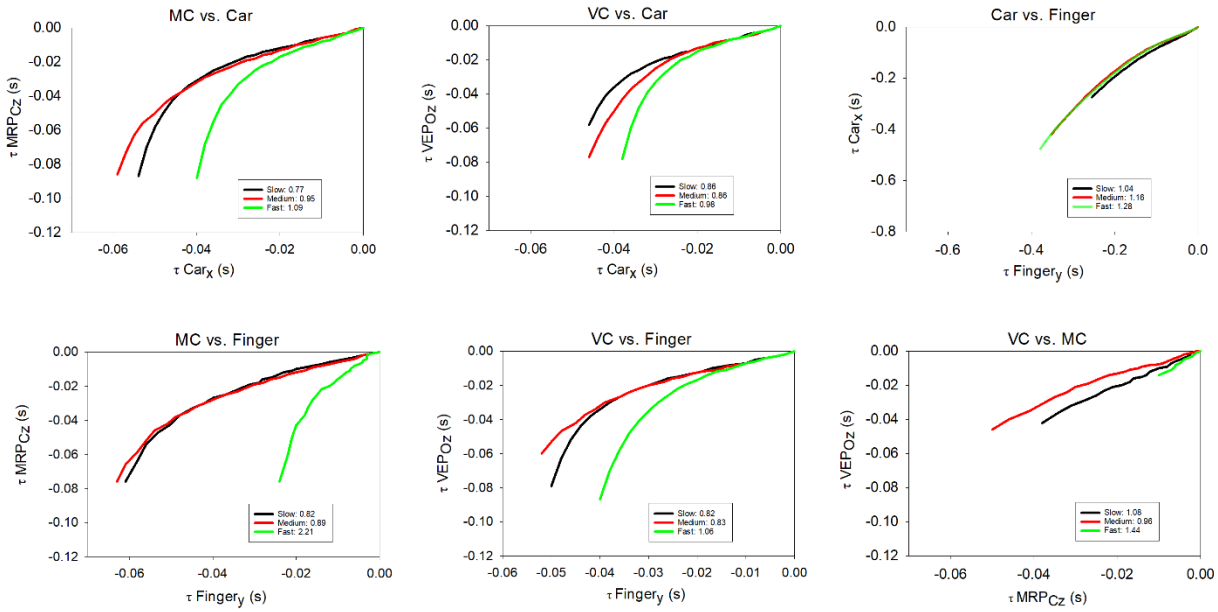

Figure 15 *– Participant 11 tau-coupling results, depicting six different tau-coupling graphs, that are thought to describe the technical and neural process of the interception task. From left to right and top to bottom, the graphs display the tau-coupling of the motor cortex and car movement, visual cortex and car movement, the car movement and finger movement, the motor cortex and finger movement, the visual cortex and finger movement, the visual cortex and motor cortex. All six graphs display an average slope height for each tau-coupling to show the difference between three different speeds – slow, medium, and fast, and how it changes in each interaction, with each coupling variable on X or Y axis.*

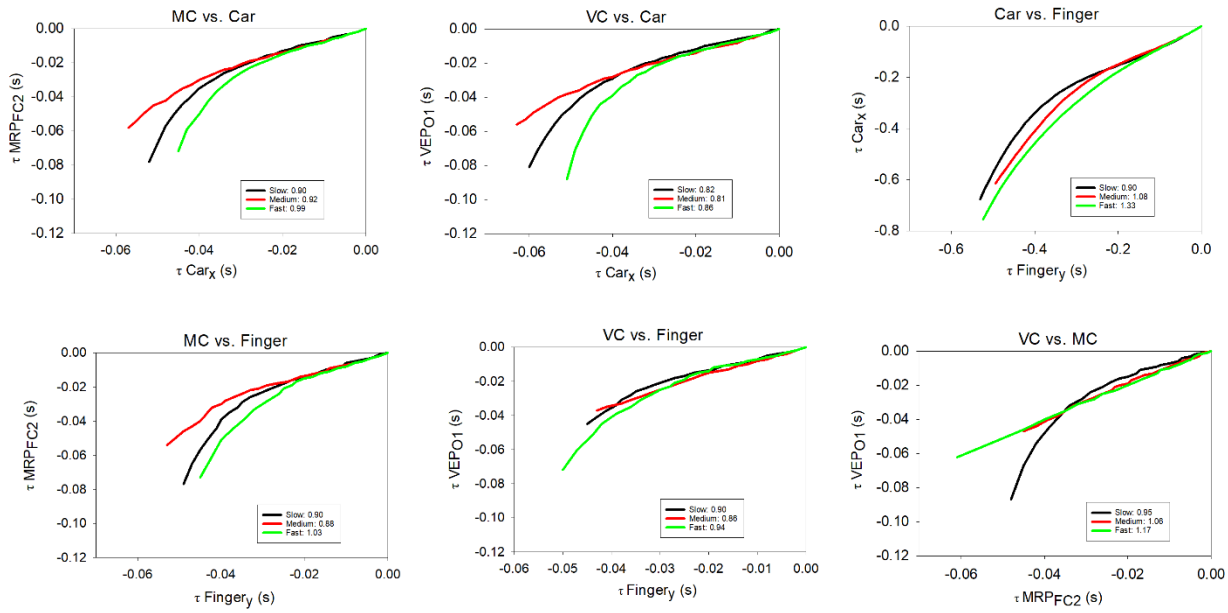

Figure 16 *– Participant 12 tau-coupling results, depicting six different tau-coupling graphs, that are thought to describe the technical and neural process of the interception task. From left to right and top to bottom, the graphs display the tau-coupling of the motor cortex and car movement, visual cortex and car movement, the car movement and finger movement, the motor cortex and finger movement, the visual cortex and finger movement, the visual cortex and motor cortex. All six graphs display an average slope height for each tau-coupling to show the difference between three different speeds – slow, medium, and fast, and how it changes in each interaction, with each coupling variable on X or Y axis.*

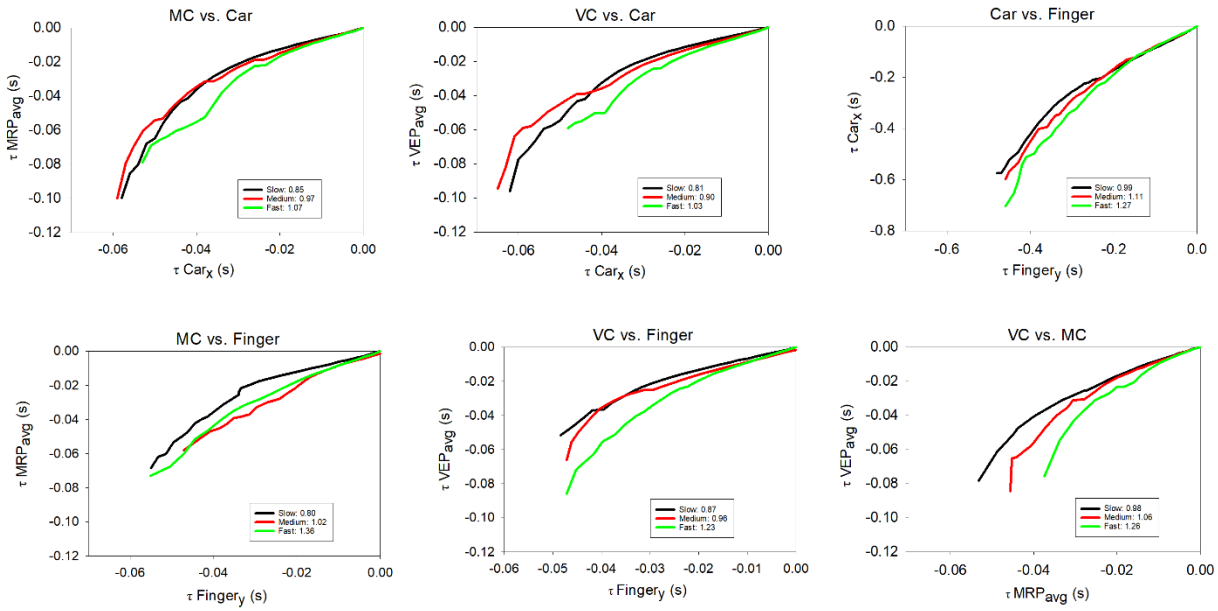

Figure 17 *– All participant average tau-coupling results, depicting six different tau-coupling graphs, that are thought to describe the technical and neural process of the interception task. From left to right and top to bottom, the graphs display the tau-coupling of the motor cortex and car movement, visual cortex and car movement, the car movement and finger movement, the motor cortex and finger movement, the visual cortex and finger movement, the visual cortex and motor cortex. All six graphs display an average slope height for each tau-coupling to show the difference between three different speeds – slow, medium, and fast, and how it changes in each interaction, with each coupling variable on X or Y axis.*

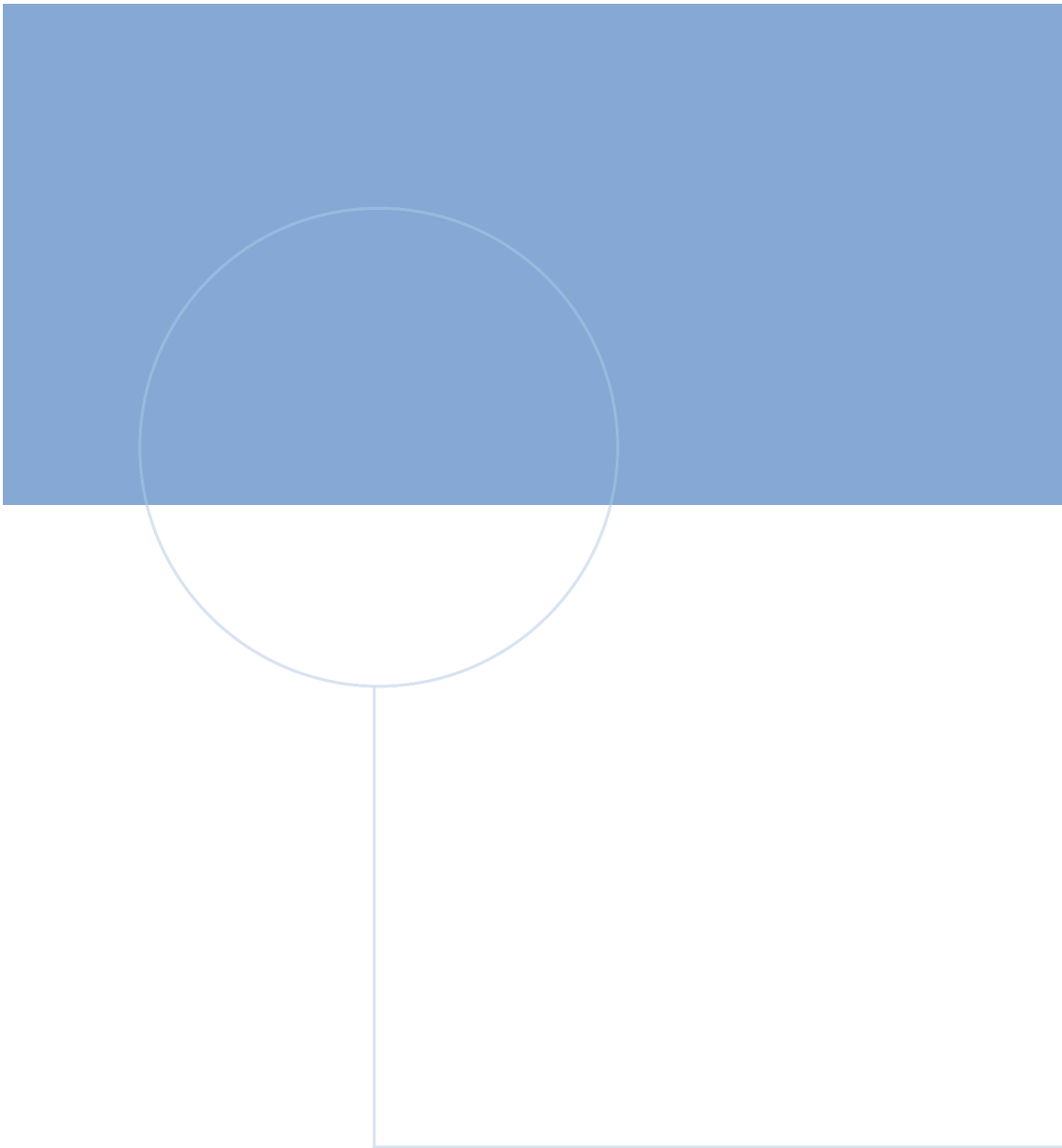

NTNU

Norwegian University of
Science and Technology